UNIVERSITY of RWANDA COLLEGE OF SCIENCE AND TECHNOLOGY ACE-ESD AFRICAN CENTER OF EXCELLENCE IN ENERGY FOR SUSTAINABLE DEVELOPMENT

University of Rwanda

College of Science and Technology

"DESIGN AND SIMULATION OF SOLAR HOME INVERTER SYSTEM SUPPORTING NONLINEAR LOAD"

A proposal submitted to the African Center of Excellence in Energy studies for sustainable development (ACE-ESD)

In partial fulfillment of the requirement for the degree of MASTER OF SCIENCE IN RENEWABLE ENERGY

By:

MUPENZI Marcellin **Ref no:221030829**

Supervisor:

Dr. Maxime BINAMA

Co-supervisor:

Dr. Antoine MUSENGIMANA

01/12/2023,

Kigali-Rwanda

Declaration

I, the undersigned, declare that this thesis is my original work, and has not been presented for a degree in the University of Rwanda or any other universities. All sources of materials that have been used in the thesis document have been fully acknowledged.

Names

Marcellin MUPENZI

Ref no. 221030829 Signature

Date of Submission: 04/12/ 2023

This thesis proposal has been submitted for examination with my approval as a university advisor.

Dr. Maxime BINAMA

Thesis Advisor Signature

Dr. Antoine MUSENGIMANA

Thesis Advisor Signature

Table of Contents

List of Figures

List of Tables

List of Abbreviations & Acronyms

A: Ampere

AC: Alternative current

ACEESD: African Center of Excellence in Energy for Sustainable Development

CSCs: Current source Converters

DMPC: Direct model predictive control

DC: Direct Current

GoR: Government of Rwanda

Hz: Hertz

HOMER: Hybrid Optimization of Multiple Energy Resources software

HF: High Frequency

I**PEM**: Integrated Power Electronics Module

IC: Integrated Circuit

MPPT: Maximum power point tracking

MOSFET: Metal oxide semiconductor field effect Transistor

MATLAB: Matrix Laboratory Software

MV-DMPPC: Multiple-Vector Direct Model Predictive Power Control

Mgs: Micro grids

NEP: National electrification plan

NST1: National Strategy for Transformation

PI: Proportional Integral

PID: proportional-integral-derivative

PV: Photovoltaic

PWM: Pulse width modulation

PCA: Power Conversion Assembly

PLECS: Piecewise Linear Electrical Circuit Simulation

RE: Renewable Energy

REG: Rwanda Energy Group Ltd

SHS: Solar Home Systems

TVs: Televisions

UR: University of Rwanda

UPS: Uninterrupted power supply

SPWM: Sinusoidal pulse width modulation

SIC MOSFET: Silicon Carbide Metal Oxide Semiconductor Field Effect Transistor

V: Volt

W: Watt

Ω: Ohm

Abstract

The growing interest in developing efficient DC to AC converters for residential use is driven by the increasing integration of renewable energy sources and the demand for energy-efficient home systems. This project involves the design and simulation of a DC to AC converter, implemented using MATLAB/Simulink and PLECS. The goal is to utilize MATLAB/Simulink and Piecewise Linear Electrical Circuit Simulation (PLECS) Software for the design, analysis, and evaluation of power electronic converters and their controllers. Focusing on enhancing energy conversion efficiency, performance, and reliability, the study aims to achieve optimal design and modeling of a domestic DC to AC converter. Specifically tailored for the requirements of renewable energy sources such as solar energy and battery storage, as well as household appliances, the proposed converter incorporates power electronics, control algorithms, and filtering methods. This research employs advanced simulation techniques to model and analyze these converter components.

A MATLAB/Simulink model was created for a closed-loop DC-DC boost converter with a broad input voltage range of 40 V to 60 V, generating a consistent 330 V DC output. The DC voltage was converted to chopped AC voltage using a 1KVA H-bridge single-phase inverter, followed by filtering to obtain a pure sinusoidal AC with an effective value of 230 V. To compare the results with standard, the simulation model has been simulated in Piecewise Linear Electrical Circuit Simulation (PLECS) Software with variable linear load and the output voltage was 220V RMS.

In the end, this project 's findings offer insightful information about how to simulate and design house DC to AC converters optimally, laying the groundwork for the creation of energy-efficient solutions that can adapt to the changing demands of contemporary domestic power systems. The findings of this project work for both cases should open the door for the widespread use of effective DC to AC conversion technology and have a significant impact on the development of sustainable energy practice in residential settings as output voltage is ranging between 220V to 230V RMS.

Keywords: DC voltage, solar pv, Simulink, Converter and Filter.

CHAPTER ONE: INTRODUCTION

1.1.Background of the Study

Energy is vital in daily life, and a country's development is often gauged by factors such as energy production and consumption. Increasing energy demands due to population growth, urbanization, and industrialization present challenges[1]. The eventual depletion of fossil fuels like coal, oil, and natural gas heightens the urgency to address the energy issue. An "energy crisis" is characterized by rising daily energy consumption and decreasing supply[2]., leading to inflation and shortages. Exploring alternative energy sources is crucial for future needs. While renewable energy, like solar power, offers environmental benefits, it may have drawbacks. Solar energy, particularly useful in remote areas, relies on photovoltaic modules and inverters to generate stable on-site electrical power from sunlight[3], [4].This output voltage of approximately 230volts AC can be used for powering small electrical appliances such as lights, radio, iron, fan etc. Most electricity consumers in the country do not make use of DC to AC converters because they are thought to be costly as compared to the level of technical profit gained through their usage. However, considering the task, this appliance can perform, it can still be considered cheap. The implementation is simple, cheaper, easy to operate and portable[5]. In this modern period where the control and monitoring of complex field operations are all based on computers, a failure of an AC power supply to communication facilities means operations stoppage, and to some small-scale industries, considerable economic and materials losses are to be sustained. It is from these backgrounds that a project entitled optimal design and simulation of home DC to AC converter has been thought to be important, as an attempt to address the above discussed problem. This project's main goal is to convert DC power that has a voltage range of 40 to 60 into 230 volt AC, which is the standard power level in electrical power grids[6]. The DC to AC converter is the focal point of this project. To do this, the appropriate oscillators, transformers, switching devices, and control circuits must be used. The converted AC can be modified using these parts to satisfy voltage and frequency specifications. Inverters are frequently used when supplying AC electricity from DC sources, including solar panels or rechargeable batteries[7].

1.2.Problem statement

According to its National Strategy for Transformation (NST1), Rwanda wants to become middle-income by 2035 and high-income by 2050. A primary goal of this approach is to guarantee that everyone has access to power by 2024. Currently, 70% of households are supposed to be connected to the national grid by the government, with the other 30% being connected off-grid. The most common supply systems available in rural areas are Automotive Generator Sets (convert mechanical energy to electrical energy through fossil fuel burning) and UPS (Uninterrupted power supply) systems. Even though all these backup supply systems perform their said functions as required, their usage still comes with different challenges, high cost and noise pollution, among others. Trying to deal with limitations of using generators as alternative or additional source of electricity, potential alternative energy sources have been explored, among which solar energy has recently caught energy players' eye.

Its audience keeps growing daily, especially with the arrival of the so-called "solar home systems" or SHS. In line with this, seeing the high rate of power outage in Rwanda, the use of solar energy is advised, but other means for uninterrupted power supply should be made available. Electric converters only convert electrical current; they do not deal with power outages on their own. Nevertheless, there is a need to investigate the integration of energy storage options such as Uninterruptible Power Supplies (UPS) in addition to optimizing the converter's design. The integration of energy storage and the DC-AC converter's efficient conversion capabilities surely enhances the system's ability to effectively handle power outages. It is to this effect that a 1kVA DC-AC power converter have been designed to produce the power that runs on 40-60 V DC batteries. This scheme is eco-friendly and produces power for a desired period.

In addition, the majority of DC to AC Converters used in renewable energy power conversion use topologies such as Bipolar Junction Transistor or BJT, POWER MOSFET and SI IGBT. These have been presented by shortcomings such as high switching loss, high power losses, and lower switching frequencies, which result in inefficiency and short lifetime of renewable energy power generation.

1.3. Main objective

To design a single-phase DC to AC converter capable of delivering 50 Hz, 230 volts, and 1000 volt-amperes of output power to a load.

1.3.1. The Specific objectives

The specific objectives of this research are as follows:

i. To provide a DC to AC converter design that reduces energy waste and operating energy for residential users while also greatly increasing energy conversion efficiency.
ii. Identify available components and design strategies to produce affordable DC to AC converters tailored for residential applications, ensuring energy-effectiveness for homeowners.
iii. Examine ways to incorporate the converter into renewable energy sources such as wind turbines and solar panels so that households can generate clean, sustainable energy more easily.
iv. Develop a fault-tolerant DC to AC converter design capable of withstanding electrical and environmental disturbances, ensuring uninterrupted power supply for residential users.
v. Investigate strategies to reduce the environmental impact of the converter, including minimizing heat generation and adopting affordable materials where possible.
vi. To ensure user safety, ensure that the converter design complies with relevant safety and performance standards, as well as electrical and safety regulations.

1.4. Research questions

The difficulties mentioned above prompt various concerns about the Rwandan grid's ability to function effectively. Among these are the following: What variables affect the inverter system's stability? How can the inverter system's performance be improved to support both linear and non-linear loads? Which techniques work best for reducing resonance problems in the LC filter so that the inverter system performs better overall? These are the questions this thesis seeks to investigate and respond to.

1.5. Scope of the study

The scope of this research is currently limited to the definitions and descriptions. The designed inverter will be used in rural area where there is no access to utility's grid and will be used in urban areas for power backup technologies, especially for lighting, cell phone charging, supplying television, Radio, computers, video recorders, life support machines and other households' equipment. The circuit was operated from 40 volt to 60-volt DC. A 48-volt battery will be used to simply generate DC Voltage. This study will be managed by using a controller (PI, or PID) in conjunction with pulse width modulation for triggering MOSFET and a second order filter LC for harmonics mitigation with a low resistance to avoid resonance. In this conversion of DC to AC, the system will produce the output of 220-230 V AC /50HZ rms for supplying both resistive and inductive loads where the system efficiency will be 95% and then the simulation of proposed system will be executed by using MATLAB/SIMULINK.

1.6. Expected outcomes.

Following are the expected outcomes at the completion of this research:

i. To design a DC/AC that support linear and non-linear loads.
ii. Future recommendation and contribution to the field will be addressed.
iii. Sensitivity analysis could be performed to identify how variations input conditions or component characteristics affect the converter's performance.

1.7. Significance of the study

This research will mainly contribute towards the enrichment of the so far available body of knowledge about optimized functionality of inverters, leading to among others the least energy DC to AC converter realization.

In addition, the sought for research findings will contribute to the academic research advancement, at the same time motivating students in technical schools to embark on entrepreneurial endeavors that not only sustain a better life standard for self, but also provide solutions to daily faced problems in the community. This work will be based on design and simulation of single-phase DC to AC converter by using SIMULINK Software.

Some details of used parameters and equipment will be provided, looking at how to convert energy stored in batteries thereafter, The supply an AC power during shortage time or in off grid area. The best alternative is using solar energy as standalone. This produces DC current, but DC appliances are very expensive and AC appliances are available on the market and affordable. Any DC to AC converter can be easily designed and implemented following the accuracy of the among all other parameters within this research.

CHAPTER 2. LITERATURE REVIEW

2.1 Introduction

An inverter is a power electronic device designed to convert direct current (DC) power into alternating current (AC) power [8]. It serves the purpose of operating AC equipment designed for standard operation and can function in reverse as a rectifier circuit, converting AC to DC power.

In modern electrical systems, inverters have found widespread applications, including power flow regulation, industrial automation, operation of electrical motors, power conditioning, harmonic compensation, and more. In the context of renewable energy sources such as solar and wind turbine systems, inverters play a crucial role in converting the generated renewable energy into AC power for integration into the grid. Additionally, inverters are commonly employed in uninterrupted power supplies (UPS), where they convert DC power to AC power at the required voltage level [9].Inverters can be categorized in various ways, with their classification often based on the type of AC waveform they produce, their ability to connect to the electrical grid, and their intended application (e.g., PV system, battery charging). The diagram below illustrates different types of inverters and their applications in microgrids.

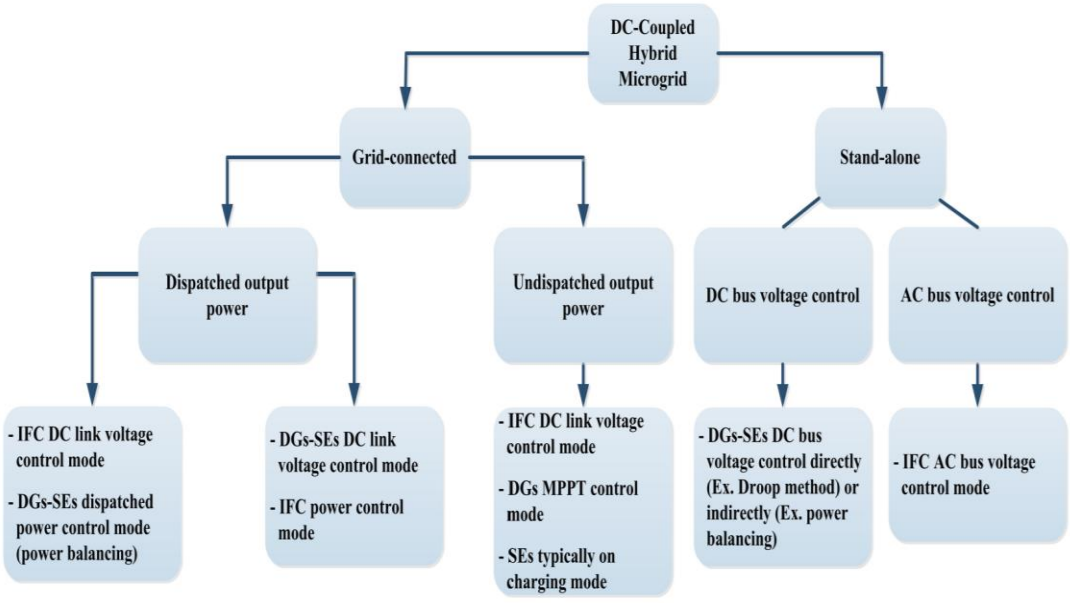

Figure 2. 1: Typical Inverter based on DC/AC [15-16].

In renewable energy, especially in PV system, the inverter is responsible for connecting the PV to the grid (Grid-connected mode) and may directly supply the power to the load (standalone PV system). By today, different countries around the world have set targets to install a certain capacity of grid-integrated or residential PV systems no later than 2050 to reduce carbon emissions [6], as the global warming caused by the green gasses affects the growth of the global economy. For instance, in China, the installed capacity of the PV system reaches 253.4 GW in 2020, far ahead of 105 GW of the 2020 target. Thus, the total installed capacity occupies 11.5% of the total electric power generation in China and 33.3% of the global PV generation capacity [7].

The case of Rwanda, 25MW, grid-connected PV farm have been installed, and high number of home-PV systems, which may occupy high percentage of the total electrical energy in Rwanda.

Besides the promising environmental benefits, there are still drawbacks to integrating PV systems into the power grid due to its fluctuation of generated power caused by intermittency and stochastic in solar irradiation and temperature. These power fluctuations ranging from under-generation to over-generation raise more concerns about power system stability and power quality problems, especially when there is a high penetration of the PV system in the power system.

Apart from the distributed grid-connected system, in some applications, especially in remote areas, where the grid extension is difficult due to economic and technical constraints, off-grid PV system are preferable to supply homes and small-industries. In real application, stand-alone PV system doesn't work alone. They may be in combination with other forms of renewable energy sources such as micro-turbines, wind generators, fuel cells, batteries. In addition, they can be found in combination with non-conversional energy such as diesel generators [10]. Square wave, modified sine wave, and pure sine wave are the three major waveforms. A more expensive power inverter uses pulse width modulation (PWM) with a high frequency carrier to approximate a sine function more closely. The quality of an inverter is described by its pulse rating. The data and a closed loop maximum power point trucker (MPPT) system are required to be gathered before applying it at any operation[8].

2.2 Overall PV-storage system configuration for the standalone system

The four main parts of an off-grid photovoltaic system are the solar panel, solar inverter, battery, and system balancing. DC current is produced by solar panels using sunlight and is subsequently stored in batteries. Included with every DC application, such as lights and fans running at 12V, is a charge controller. There are three primary categories for solar PV power systems: off-grid, often called stand-alone systems; on-grid, sometimes called grid-tied or grid-connected systems; and hybrid, which is a grid-connected system with battery storage. The off-grid solar system's configuration is shown in Figure 2.2.

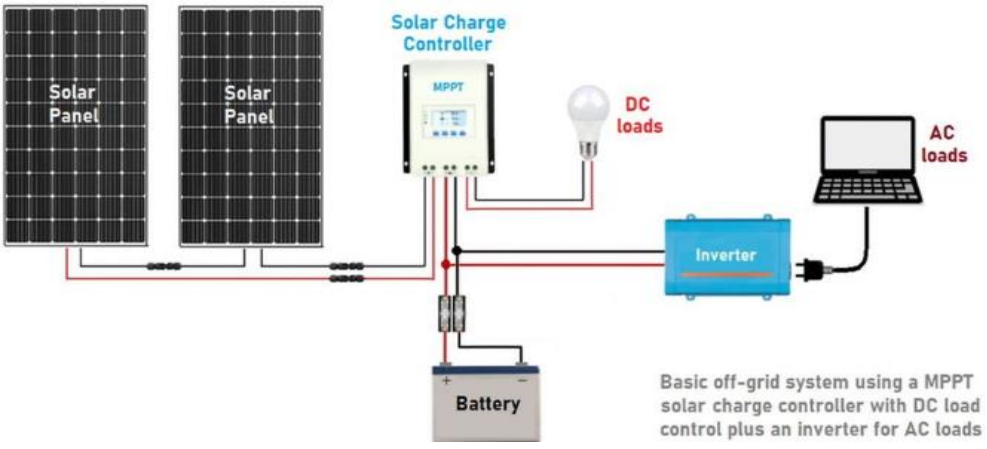

Figure 2. 2:OFF Grid solar system[11].

This configuration can power several home appliances, including fans, air conditioners, refrigerators, water pumps, and televisions. A 1 kW off-grid solar system is adequate for a home with two to four bedrooms. On the other hand, a 3 kW off-grid solar system might be suitable if your water pump is 1 HP. An efficient option for powering an air conditioner is a 5-kW solar system. Business installations like a store, clinic, small mill, or gas station should use a 10 kW off-grid solar system[11].

2.2.1 Operation of the off-grid PV-storage system

The solar panels, which are composed of photovoltaic cells that transform sunlight into direct current (DC) electricity, are the main component of a standalone PV system. The charge controller, which controls how quickly the storage batteries charge, oversees this electricity. The batteries store electrical energy as chemical energy for use when more electricity is required or during times when there is no sunlight. An inverter converts the direct current (DC) that is stored in the batteries into alternating current (AC) when electricity is required. At the installation site, this AC current provides clean, sustainable energy by supplying electrical equipment and devices[12].Compared to conventional inverters, PWM-based inverters have many more protection and control circuits[13].

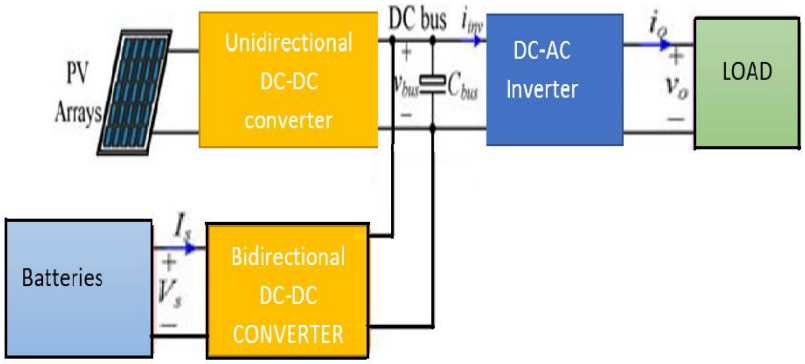

Figure 2. 3:System configuration with details of Power supply and converter

In this setup, electricity from the PV arrays is transferred to the DC bus via the unidirectional DC-DC converter at the front end.

Power transfer between the storage units and the DC bus is facilitated by the bidirectional DC-DC converter, and the intermediate DC bus voltage is converted into the necessary AC voltage for the load by the DC-AC converter.

Interest in stand-alone systems has increased as energy storage and photovoltaic solar systems gain prominence. The main components of a standalone photovoltaic system are batteries for energy storage, an inverter, a charge controller, and solar panels. A thorough explanation of each part is provided, with special attention to the bidirectional DC-DC converter[14]. According to the figure 2.4 configuration, the circuit for the energy management system is a bidirectional buck/boost DC/DC converter.

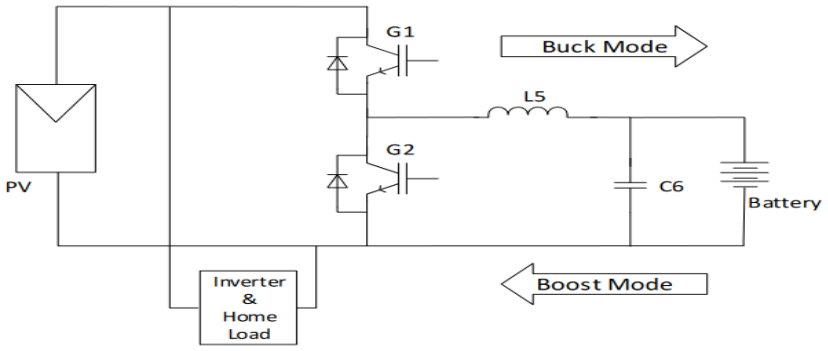

Figure 2. 4: Topology of bidirectional buck-boost converter [15].

This circuit topology operates in either boost mode (battery discharging) or buck mode (battery charging), and the modes are explained as follows: In boost mode, the G2 gate pulse is high, turning on the Insulated Gate Bipolar Transistor (IGBT). G1 can be in one of two states during this mode: State 1, where G2 is high and G1 is low, indicating a short circuit in the DC/DC converter, causing the inductor L5 to charge from the battery voltage; and State 2, where G2 is low and G1 is low, indicating that the DC/DC converter is in an open circuit, and the inductor voltage is in series with the DC link voltage, leading to the charging of C6 and a boosted output voltage. In buck mode, the IGBT is turned on, and the G1 gate pulse is high. G2 can also be in one of two states in this mode: State 1, where the battery is charged by capacitor C6 and inductor L5 as G1 is high and G2 is low; and State 2, where both G1 and G2 are low, causing the voltage across the battery to step down, and the inductor is discharged across the freewheeling diode[15].

Regarding PV panels (solar energy), the number of solar panels must ensure sufficient energy production to meet the required demands and recharge the batteries during the designated sunlight hours. The charger controller/inverter should align with the installed solar panels and batteries, and its output should match the system's electrical power requirements, such as instantaneous power. Concerning batteries, they must have the capacity to support the specified instantaneous and consumption electrical power as outlined in the design. They should be capable of supplying instantaneous power to meet the house's kW load and sufficient storage to ensure a continuous and reliable power supply aligned with the house's demands[16]. Energy storage is a crucial component for a standalone house to guarantee a consistent and dependable power supply.

2.2.2 Maximum Power Point Tracking.

Typically, only thirty to forty percent of the total solar light that a panel receives can be used to generate power. One method of increasing a specific solar panel's efficiency is to use Maximum Power Point Tracking, or MPPT for short. The Maximum Power Point Tracking (MPPT) technique is used to maximize photovoltaic (PV) power under circumstances. A photovoltaic panel's maximum power production is determined by several elements, including solar radiation, ambient temperature, and cell temperature. MPPT, is determined by comparing the output of a specific PV panel with the battery voltage and determining which voltage is the most efficient[17].The MPPT controller have program of perturb and observe algorithm so that microcontroller always try to sense an input signal parameter that have fed to it and trying to get the output that have equal to load input range[18].

The power generated by the PV panel is variable in nature and varies with the state of the atmosphere. Therefore, to optimize the power extracted from a PV at its maximum and it is depicted in Figure 2.5[19].

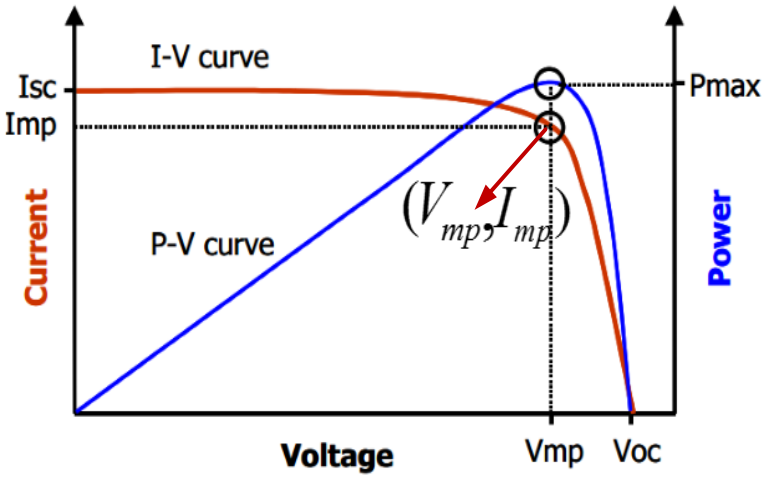

Figure 2. 5:The curves of I-V and P-V of photovoltaic device [53]

2.3 Stability analysis of stand-alone inverter

The stability of the inverter system can be investigated in a number of ways, the most popular of which is tiny signal stability analysis. Bode diagrams and root contours are evaluated in this analysis[20]. To verify the overall stability of the inverter system theoretically, root contour and Bode diagram evaluations were performed. The DC/AC converter is controlled in cascaded loop, with inner loop responsible for current regulation and outer loop responsible for stabilizing the load voltage to a predefined level [21].

2.4 Overview on DC to AC converter

An inverter's small size and light weight are essential for several uses. The application of a high-frequency (HF) link inverter topology can accomplish this. An illustration of this is the DC/DC converter type, in which a bridge inverter converts the direct input voltage into an HF square wave, which is then filtered and rectified. The need for a light and relatively small inverter is important for a variety of applications, and the DC/DC converter type of high-frequency (HF) link inverter topology is one way to meet these needs. Depending on particular design requirements, DC-AC converters convert DC input voltage into AC output voltage and frequency. They are used to change the waveform of the DC input to AC. The most common inverter used for this purpose is the H-Bridge, which is regarded as a typical DC-AC converter. In order to implement a pure sine wave inverter, the author has presented the topology of a voltage source inverter (VSI) [32].Based on quadrant operation, H-Bridge has various operating modes.

Table 2. 1: Summary of the DC/AC converters

Type of converter	Description	References
Grid-Tied Inverters	Connect renewable sources to the grid, convert DC to AC, and may allow feeding excess power into the grid.	[29]
Off-Grid Inverters	Designed for standalone systems not connected to the grid, convert DC to AC for appliances in off-grid homes or remote locations.	[28]
Microinverters	Convert DC power from individual solar panels into AC power, offer individual panel monitoring and improved energy harvest.	[30],[31]
String Inverters	Used in solar panel arrays, where multiple panels are connected in series (a string) and convert combined DC power into AC power.	[30],[31], 14]

2.5 Overview of Battery and Energy Management on PV

A backup battery storage system should be included in the PV system's design. In this system, MPPT control is achieved by means of a DC-DC boost converter. In addition, the system has a battery backup to guarantee that it will continue to function even if it is unable to supply the necessary loads or keep the microgrid's voltage and frequency stable. A variety of converters, such as DC/DC and DC/AC converters, are included in the energy storage system. Since that PV arrays provide DC electricity, a DC-DC converter is commonly used in this situation to modify the voltage level[61]. In additional the boost-buck converter is very vital and compulsory because of it is capable to accomplish the both tasks of charging and discharging system of battery and protect battery in order to overcome the system of overcharging and discharging in order to increase battery life condition[62].

In order to inject or absorb active power via a bidirectional DC-DC converter that operates in the buck mode, a battery is connected in parallel to the PV array. If the battery is also supplying power

to the system or utility grid, it operates in the boost mode as long as it is connected to the system, and the control signal that is given to the converter switches maintains the operation mode. Because distributed generators that use renewable energy are erratic and unpredictable, managing and operating a renewable micro grid presents numerous challenges. As a result, the PV module must have energy storage[63].

2.6 Available Types of Battery Storage

Lead-acid batteries were the predominant economically viable battery technology until recently. But now that it's commercially feasible, an improved valve-regulated lead-acid battery is becoming more and more used in utility systems. New battery technologies with varying sizes and degrees of utility operating readiness, like zinc/bromide and lithium-ion, are currently in different phases of development. There are currently the following battery kinds available on the market:

- Lead-Acid Battery
- Controlled by a valve Lead-Acid (VRLA) Battery
- Battery with Vanadium Redox Flow (VRB)
- Battery with Sodium Sulphur (SSB)
- Battery Type: Polysulfide Bromide Flow (PSB)

Those type of battery has different advantageous and disadvantageous, but everyone can choose one type of battery according to their research but in uninterruptible power supply system but, the battery applications are mostly used to reserve power in interruptible power supply system (UPS). Eventually lithium-ion battery ($Li-Ion$) has the following advantages compared to other batteries in general it has the following advantages:

- High energy density which is the range of$(300-400\ kWh/m^3)$,$130kWh/ton$.
- High efficiency approximately near of 100%.
- Long cycle life.
- It is in-expensive[64].

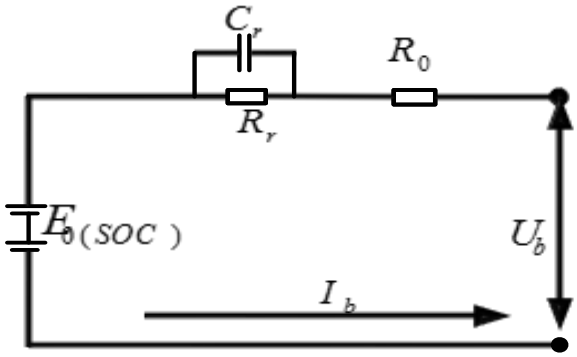

Figure 2. 6:Equivalent circuit of battery

With the right parameter selection for deep cycle applications, the battery in this simulation is modeled as a lead acid battery. There are some presumptions that the lead acid battery has a 20% discharge capacity and an 80% charge capacity. The two primary equations used to describe battery charge and discharge models are found in battery models.

The equations of discharge and charge can be written as follow:

$$V_{Battery} = V_0 - R.i - \frac{KQ}{(Q-it)}(it + i^*) + Exp(t) \qquad (2.1)$$

$$= V_0 - R.i - \left[K\frac{Q}{i.t - 0.1Q}\right]i^* - \left[K\frac{Q}{Q - it}\right] \qquad (2.2)$$

The following formula is significant: $(V_{Battery})$ is the battery voltage; V_0 is the constant voltage of the battery (V); K is the polarization constant (V/Ah) or polarization resistance Ω).Q is the battery capacity (Ah); it is the integral of idt, signifying the actual battery charge (Ah); A is the exponential zone amplitude (V); B is the inverse of the exponential zone time constant (Ah^(-1)); R is the internal resistance (Ω); i is the battery current (A); and i* is the filtered current (A) [65].

$$C = I^P t \qquad (2.3)$$

Where C is the battery capacity (Ah), I is the discharge current (A), P is the peukert's constant is varying between 1.1 and 1.3 for lead acid battery.

As aforementioned, that battery side with two-way DC/DC parallel with photovoltaic cells on side of DC bus, so the use of two -way DC/DC buck. Buck and Boost discharge control for the battery.

The set D duty cycle is exclusively reserved for step down and step up voltage module due to the switching on duty cycle, so Boost and Buck mode corresponding to the steady state. Generally, the equations regarding voltage in terms of duty cycle are determined as follow:

$$\begin{cases} U_c = D_{dutycycle.} U_{dc} \\ I_C = \frac{1}{Dutycycle} I_{dc} \end{cases} \quad (2.4)$$

$$\begin{cases} \mathrm{U_{dc}} = \frac{1}{1-\mathrm{D_{dutycycle}}} \\ \mathrm{I_{dc}} = \left(1 - \mathrm{D_{dutycycle}}\right).\mathrm{I_c} \end{cases} \quad (2.5)$$

2.7 Research gaps

Energy storage systems are widely used in many different applications, including electric cars, microgrids, renewable energy sets, and continuous power supply. Still in Rural Areas the converter is required for AC equipment which is also increasing in this modern Technologies. However, much research works on implementation of DC-AC converter, however still further research is needed to improve the performance of the inverter under load Variation.

CHAPTER THREE. METHODOLOGY

3.1. Introduction

The low pass filter was designed with the inverter's stability analysis in mind. During the simulation, the bode diagram in terms of magnitude and phase angle indicates the system's stability in relation to the input and variation. Irrespective of the grid parameters or the specified values for active and reactive power, the inverter current is constrained to remain below a predetermined threshold. Nevertheless, the stability of the closed-loop system will be engineered to ensure convergence toward a designated equilibrium point.

3.3 Research step

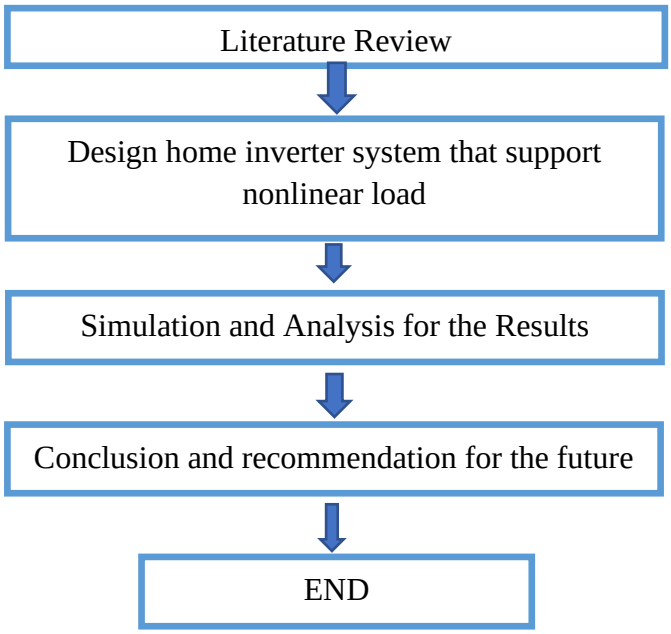

Figure 3. 1: Research steps

The main aim of this research is to improve the design, simulation, stability analysis with validation of a DC to AC converter for household use.

The growing demand for reliable and efficient household energy systems emphasizes the significance of converter design advancements. The primary objectives of this study are fourfold: First, create an optimal mathematical model for the DC to AC converter, including critical parameters such as inductance, capacitance, resistance, and control variables; second, simulate the

designed converter using MATLAB/Simulink, specifying simulation parameters and evaluating performance under various conditions; and third, conduct stability analysis using state space matrices and Bode diagrams to evaluate the converter's stability under divergent conditions, levees, and voltages.

3.2 Modelling and Stability Analysis

This study's primary goal was to create a standalone inverter that could handle both linear and nonlinear loads. We looked at the significance of control loop parameters as well as the dynamic performance of the recommended control strategies. To accomplish the objectives of the study, we first built a mathematical model that represented the power stage and control system dynamics of the inverter system.

This model was then used, using a small signal stability technique, to evaluate the stability resilience and performance of the inverter system under various load conditions[67].

3.3 State-Space Model

Compared to other approaches, the state-space modeling method has been widely used in power system modeling due to its numerous advantages, including ease of implementation, adaptability to any harmonic, and simplicity in frequency domain transformation. Nonlinear differential equations can be used to represent the model encapsulating the system's dynamic behavior, as shown in equations 3-1.

$$\begin{cases} \dfrac{\mathrm{d}\boldsymbol{x}(\boldsymbol{t})}{\mathrm{d}\boldsymbol{t}} = f\left(\boldsymbol{x}(\boldsymbol{t}), \boldsymbol{u}(\boldsymbol{t})\right) \\ \boldsymbol{y}(\boldsymbol{t}) = g\left(\boldsymbol{x}(\boldsymbol{t}), \boldsymbol{u}(\boldsymbol{t})\right) \end{cases} \tag{3.1}$$

where $\boldsymbol{x}(t)$, $\boldsymbol{u}(t)$ and $\boldsymbol{y}(t)$ are the state, input, and output vector respectively, given by:
$\boldsymbol{x}(t) = [x_1(t), x_2(t), \ldots x_n(t)]^T$, $\boldsymbol{u}(t) = [u_1(t), u_2(t), \ldots u_r(t)]^T$ and $\boldsymbol{y}(t) = [y_1(t), y_2(t), \ldots y_p(t)]^T$.

The indices n, r, and p represent the number of variables, input variables, and output variables, respectively. In accordance with this research, the nonlinear model representing the system under consideration may include the inverter system's control system, load, and inverter power section.

Due to the difficulty of analyzing the nonlinear model in Eq. 3-1, the nonlinearities in the system in Eq. 3-2 are reduced for small-signal analysis by linearizing it around the steady-state operating point obtained by solving the system equations in Eq. 3-2 when the derivative terms are zeroed. The resulting linear time-invariant system, as shown in Eq. 3-2, can be expressed in terms of a generalized model[68].

$$\begin{cases} \dfrac{\mathrm{d}\Delta \boldsymbol{x}(t)}{\mathrm{d}t} = \boldsymbol{A}\Delta \boldsymbol{x}(t) + \boldsymbol{B}\Delta \boldsymbol{u}(t) \\ \Delta \boldsymbol{y}(t) = \boldsymbol{C}\Delta \boldsymbol{x}(t) + \boldsymbol{D}\Delta \boldsymbol{u}(t) \end{cases} \tag{3.2}$$

where A, B, C, and D are the system state-space matrices, with dimensions nxn,nxr,pxn, and pxr, respectively. Δ denotes the small deviation from the steady state.

Using various techniques, the state-space model obtained in Equation 3-2 can be used to analyze the system's stability performance under various operating conditions. The Bode plot stability analysis technique, eigenvalue stability analysis, and impedance-based stability analysis are explained in [68, 69].

3.4 Eigenvalues Stability Analysis

The eigenvalue method was chosen for the stability analysis because it can provide critical information about the source of oscillation modes and damping properties at various frequencies [69]. Furthermore, it provides a straightforward method for examining the impact of system characteristics on stability. The eigenvalues of the system matrix A, which specify the system's dynamic behavior based on the small-signal model given in Equation 3-3, are examined to determine the system's stability. This analysis is based on the system's characteristic equation, which is obtained from Equation 3-3, and is informed by the information provided by the control system[64,69].

$$\det(\boldsymbol{A} - \boldsymbol{\lambda I}) = 0 \tag{3.3}$$

with $\boldsymbol{\lambda} = [\lambda_1, \lambda_i, \ldots, \lambda_n]$ is the system eigenvalues vector of $\boldsymbol{A}$. The characteristic eigenvalues of the system are expressed in Eq. 3-4.

$$\lambda_i = \sigma_i \pm j\omega_i \tag{3.4}$$

Here, λi represents the system's i^{th} eigenvalue, whereas σi stands for its real portion and ωi for the

ith eigenvalue's distinctive angular frequency.

The imaginary part of the eigenvalue clearly represents the oscillation frequency in Hertz, whereas the real component indicates the damping of the system oscillation. Using the system eigenvalues, equations 3-5 and 3-6 provide precise definitions for the oscillation frequency (fi) and damping ratio (i) of the modes.

$$f_i = \frac{\omega_i}{2\pi} \tag{3.5}$$

$$\zeta_i = -\frac{\sigma_i}{\sqrt{\sigma_i^2 + \omega_i^2}} \tag{3.6}$$

Only when all real components of the system's eigenvalues are negative (σi < 0) is the system considered stable.

In a root-locus representation, this requirement corresponds to all system eigenvalues being on the left side of the s-plane. If any eigenvalue has a positive real part, it indicates a negative damping ratio and leads to instability. If there are complex eigenvalues (i 0), which are always found in conjugate pairs, the system can oscillate if their imaginary parts are close to the imaginary axis (y-axis), implying that the damping ratio for dominating eigenvalues is low. If and only if the real part of the critical eigenvalues is zero (σi = 0), the system reaches critical instability[69].

3.5 Bode Plot Stability Criterion

Starting with the system given by Equation (3-2), one can derive the system's transfer function. The Bode plot for the system transfer function is examined using the Bode Plot Stability Criterion to evaluate the system's stability. This criterion assesses system stability thoroughly by considering the gain and phase properties of the system response. The Bode Plot Stability Criterion is widely accepted as the best method for assessing system stability[70].

3.5.1 Gain and Phase Margins

Gain margin and phase margin are two essential stability metrics that are introduced by the stability evaluation in the Bode plot. The amount of extra gain that can be added to a system without causing instability is known as gain margin. On the other hand, phase margin represents the amount of additional phase shift that can be used without causing instability.

Phase margin and gain margin are two critical stability indicators, and the Bode plot stability

criterion emphasizes their importance. Whereas the gain margin indicates the excess gain that can be used in a system without creating instability, the phase margin indicates the excess phase shift that can be added to a system without creating instability.

3.5.2 Determining Stability Using Bode Plots

The Bode plot stability criterion evaluates the stability of a system based on positive gain and phase margin values. A system is deemed stable when both the gain margin and phase margin are positive. Conversely, if either the phase margin or gain margin is negative, the system is regarded as unstable. This criterion is widely employed in control system analysis due to its capability to offer a quantitative evaluation of system stability[70].

The depiction of phase margin and gain margin is presented in the figure below.

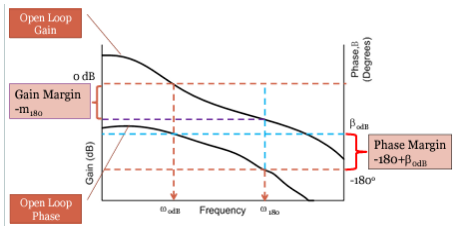

Figure 3. 2: Schematic Bode diagram

Specify two frequencies: w_0 dB represents the frequency at 0 dB gain, and w180 denotes the frequency of -180-degree phase shift. • The stability of the control system is affirmed when both the gain margin (GM) and the phase margin (PM) are positive. • The control system is marginally stable when both the gain margin (GM) and the phase margin (PM) are zero. • If either the gain margin (GM) and/or the phase margin (PM) are negative, the control system is deemed unstable[70].

CHAPITER 4: INVERTER- PV – BATTERY SYSTEM SIMULATION

4.1. Introduction

The Figure 4.1, shown is composed by the inverter, DC-DC converter and LC filter responsible for transferring the power generated from PV generator to the load. The battery storage is required to supply the power to the load when the generation doesn't meet the load power or store the energy if the generation surpass the load needs. The power to or from battery is transferred through a back boost converter controlled to stabilize the DC-link voltage to a constant level.

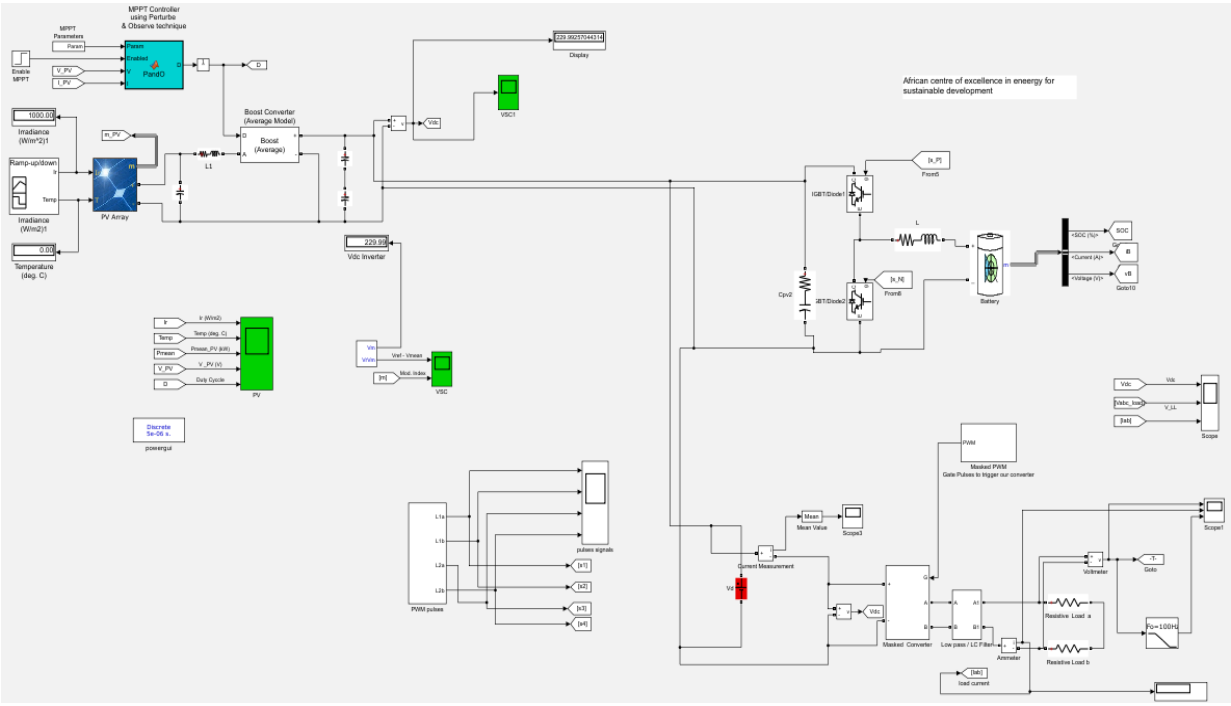

Figure 4. 1: Main circuit

4.2. PV Source simulation

PV Array block implements an array of photovoltaic (PV) modules. The array is built of strings of modules connected in parallel, each string consisting of modules connected in series and parallel to form an appropriate output voltage and power. The output power of the solar panel is intermittent and uncertainty, it alters according to the variations of solar irradiation levels and ambient temperature.

In order to have maximum power from the solar panel at any instant. The parameters considered during the simulation are: Open circuit voltage Voc (V) is 64.2V, Voltage at maximum power point Vmp (V) is 54.7V, Temperature coefficient of Voc (%/deg.C) is -0.27269 %/deg.C.

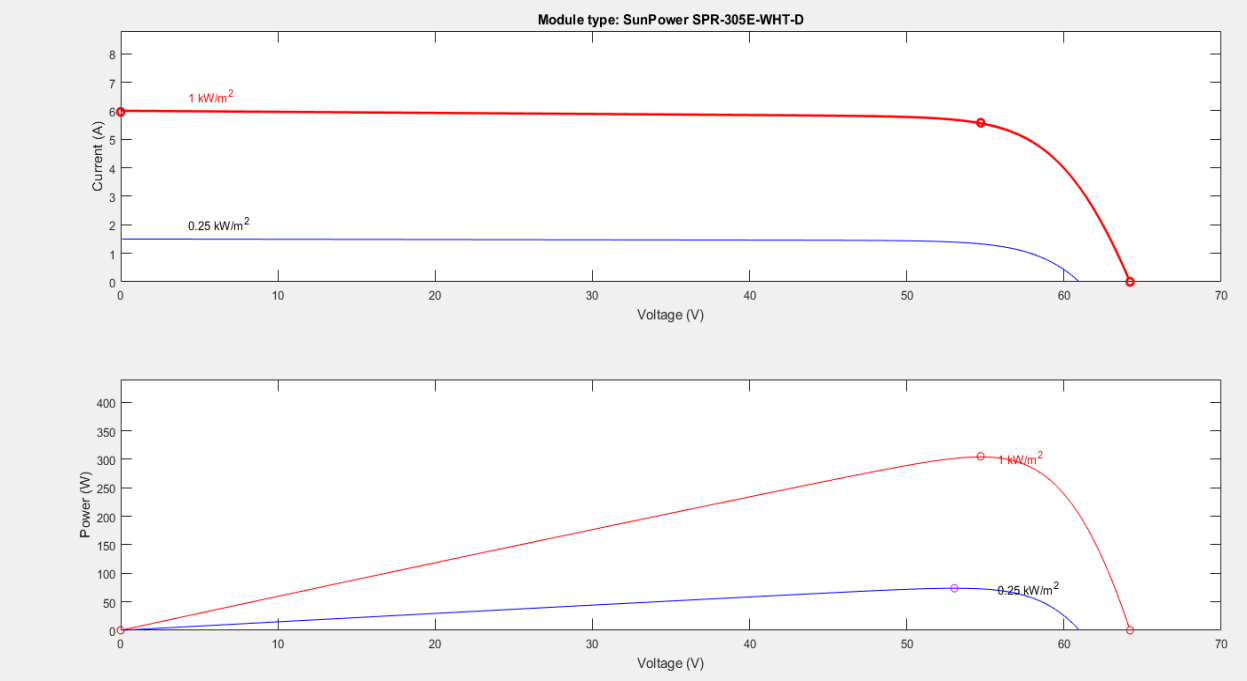

Figure 4. 2: Characteristic of PV

The PV source characteristic during simulation provide both current in function of voltage and the power outpour in function of voltage. The maximum put out Power and current are 300 and 6A at 1kw/m^2, Respectively.

4.3. Battery simulation

Battery is modeled as a nonlinear voltage source whose output voltage depends not only on the current but also on the battery state of charge (SOC), which is a nonlinear function of the current and time. The voltage of battery Vb is described by the follow equation[73]

$$\text{Vb}=V_O - R_b I_b - K\frac{Q}{Q-\int I_b dt} + A * Exp(-B \int I_b dt) \quad (4.1)$$

$$\text{Soc}=100\left(1-\frac{\int I_b dt}{Q}\right) \quad (4.2)$$

Where Rb internal resistance of battery, Vo is constant open circuit voltage, Ib is battery current, K polarization voltage, Q battery capacity in Ah, A is exponential voltage in and B exponential voltage in $(Ah)^{-1}$. To find the result shown below, the following parameters was put in software: Nominal voltage is 48V, rated capacity is 50Ah, initial state-of-charge is 45%, maximum capacity is 54Ah, Cut-off Voltage is 49V, fully charged voltage is 50V and nominal discharge current is 21.35 A

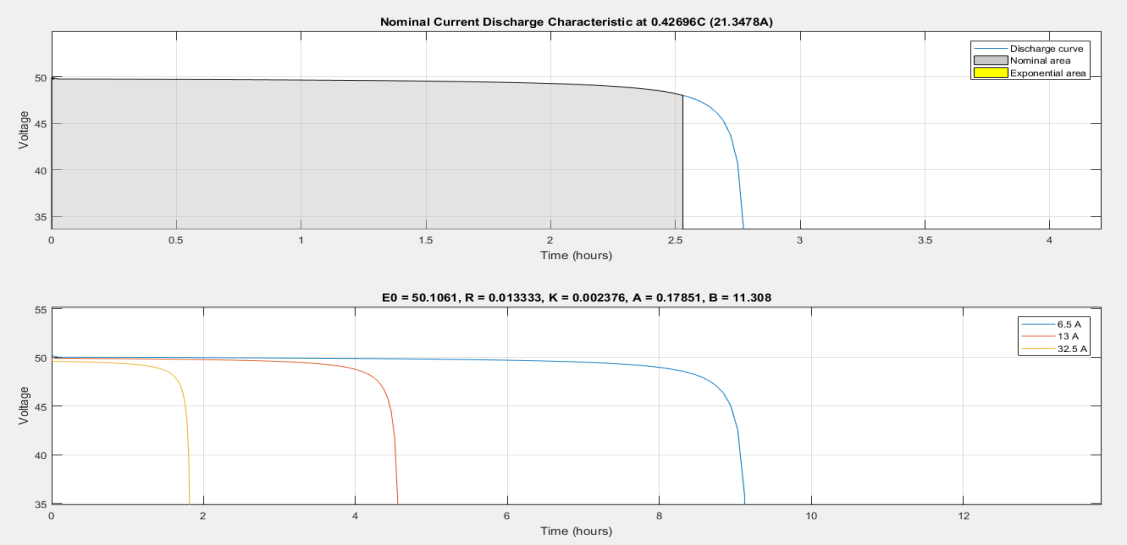

Figure 4. 3: Characteristic of battery.

4.4 Booster converter

A boost converter or step-up converter is a DC-to-DC converter that increases voltage, while decreasing current, from its input (supply) to its output (load). It is a class of switched-mode power supply (SMPS) containing at least two semiconductors, a diode and a transistor, and at least one energy storage element: a capacitor, inductor, or the two in combination. To reduce voltage ripple, filters made of capacitors (sometimes in combination with inductors) are normally added to such a converter's output (load-side filter) and input (supply-side filter).

The key principle that drives the boost converter is the tendency of an inductor to resist changes in current by either increasing or decreasing the energy stored in the inductor magnetic field. In a boost converter, the output voltage is always higher than the input voltage.

To express the mathematical modelling of input voltage and output voltage in function of duty cycle, the two mode of operation I and II are required.

At mode I if the switch is closed $\Delta IL = \frac{Vin}{L} DT$ (4.3)

At mode II one is open $\Delta IL = (\frac{Vin-Vout}{L})(1-D)T$ (4.4)

Since the net change in current through the inductor in one complete cycle is zero i.e. the summation of the rate of change of current in Mode I and Mode II becomes zero

$$\Delta IL\ (Mode\ I) + \Delta IL(Mode\ II) \quad (4.5)$$

$$\frac{Vin}{L} DT + \frac{Vin-Vout}{L})(1-D)T = 0 \Rightarrow \boldsymbol{V_O = \frac{V_{in}}{1-D}} \quad \textbf{(4.6)}$$

Where Vo,Vin and D are output voltage ,input voltage and Duty cycle Respectively

4.5 Open loop simulation of DC-DC Converter

An open-loop simulation in the Matlab/Simulink environment was carried out using the DC-DC boost converter design parameters that were input into the software, as shown on Figure 4.4. The input supply voltage is systematically adjusted in increments of 40 V and 60 V, ranging from 40 V to 60 V. The resulting open-loop output voltage and current are illustrated in Figure 4.22.

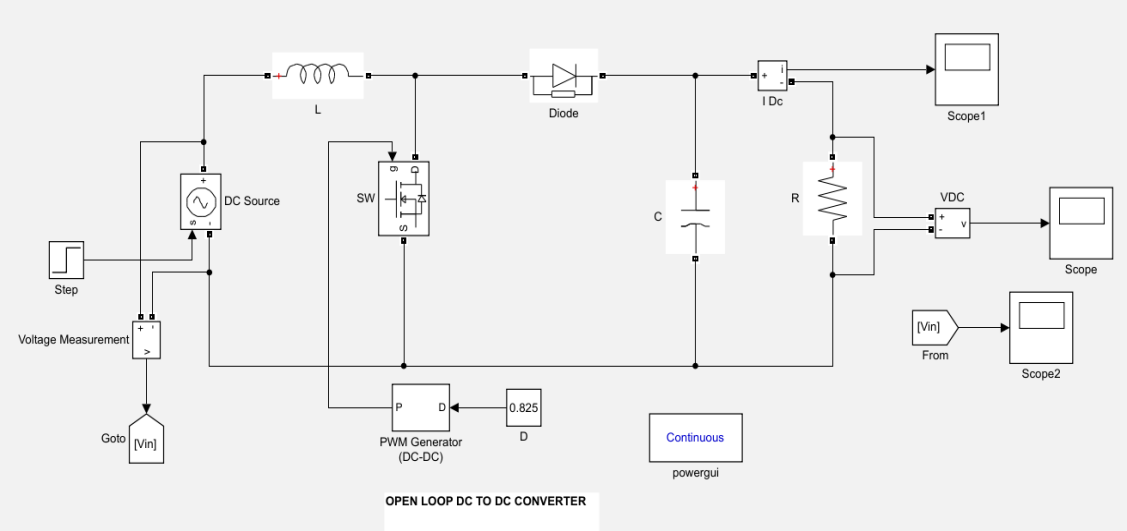

Figure 4. 4:Open loop control system

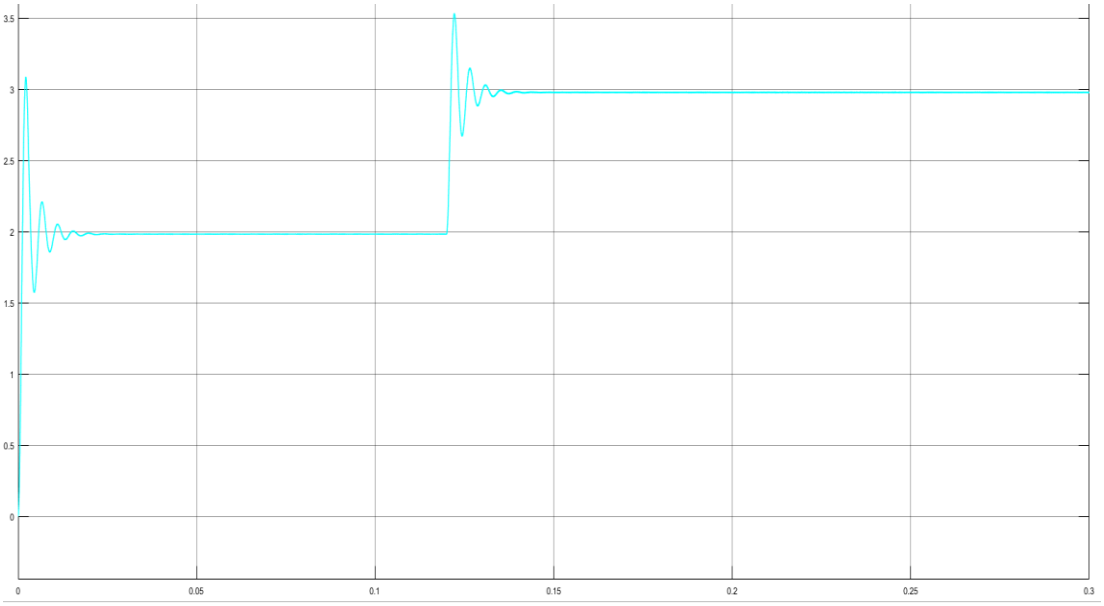

Figure 4. 5: Output current with two step

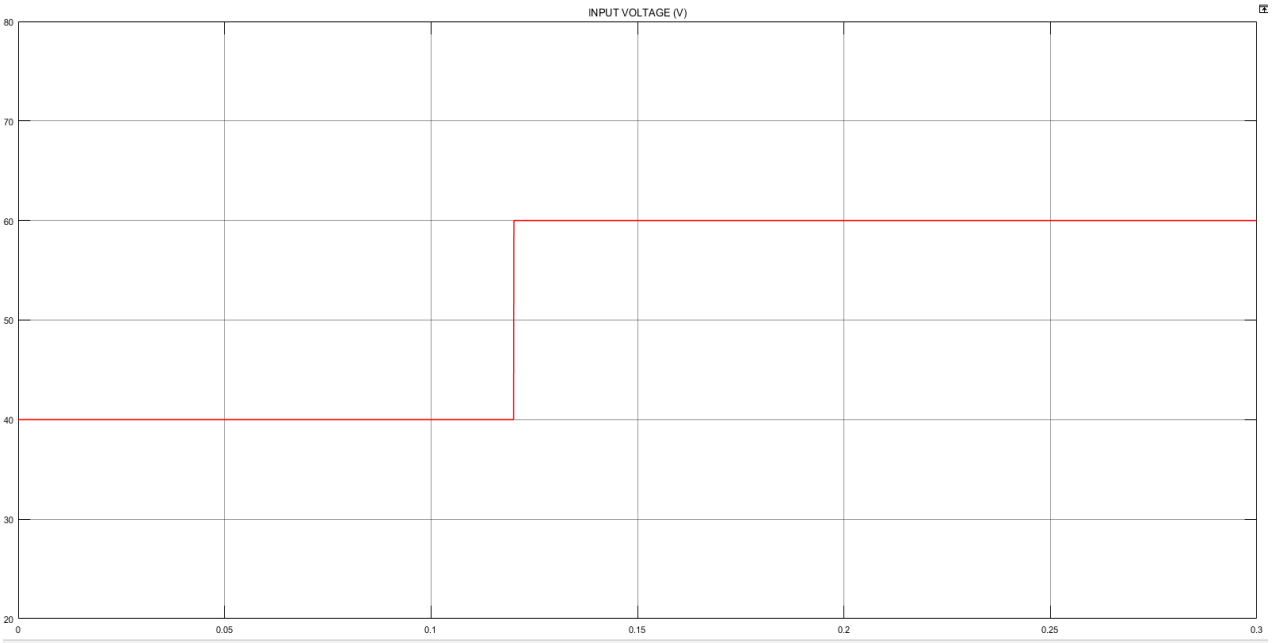

Figure 4. 6:Input voltage range

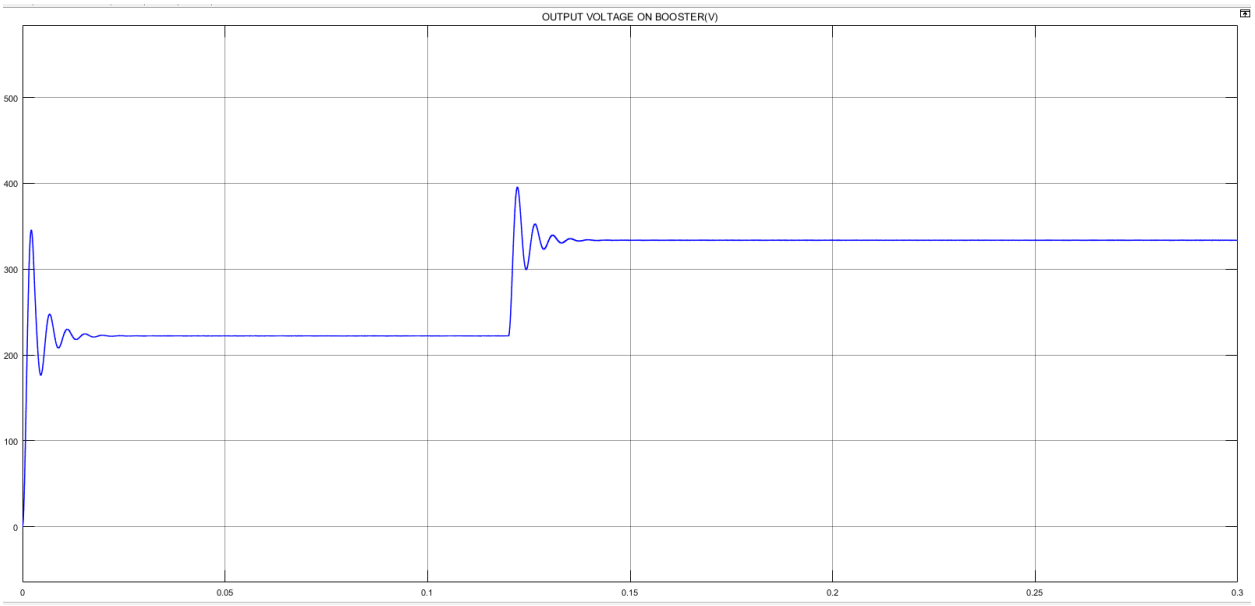

Figure 4. 7:Out Put Voltage for open loop DC to DC boost

4.15 Closed loop simulation of DC-DC Converter

Using MATLAB's PID auto-tuning tool, a PID controller was designed to govern the variable supply voltage from the solar PV panel. The closed-loop simulation (Fig. 4.8) shows that the boost converter maintains an output voltage of 330 V DC even under varying supply voltages of 40 V and 60 V (Fig. 4.6).

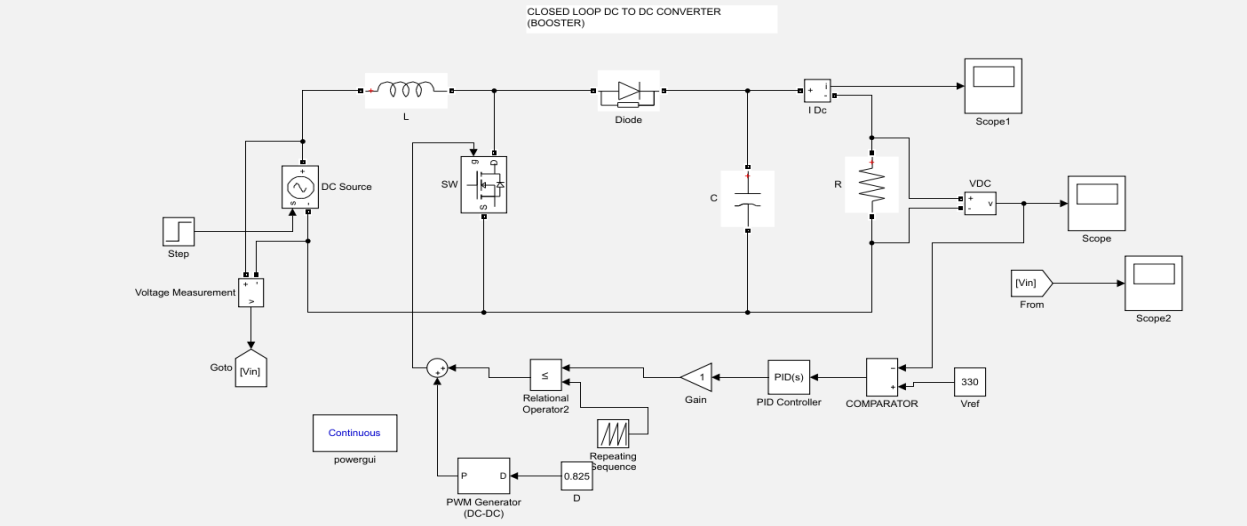

Figure 4. 8:Closed loop control system with dc-to-dc converter

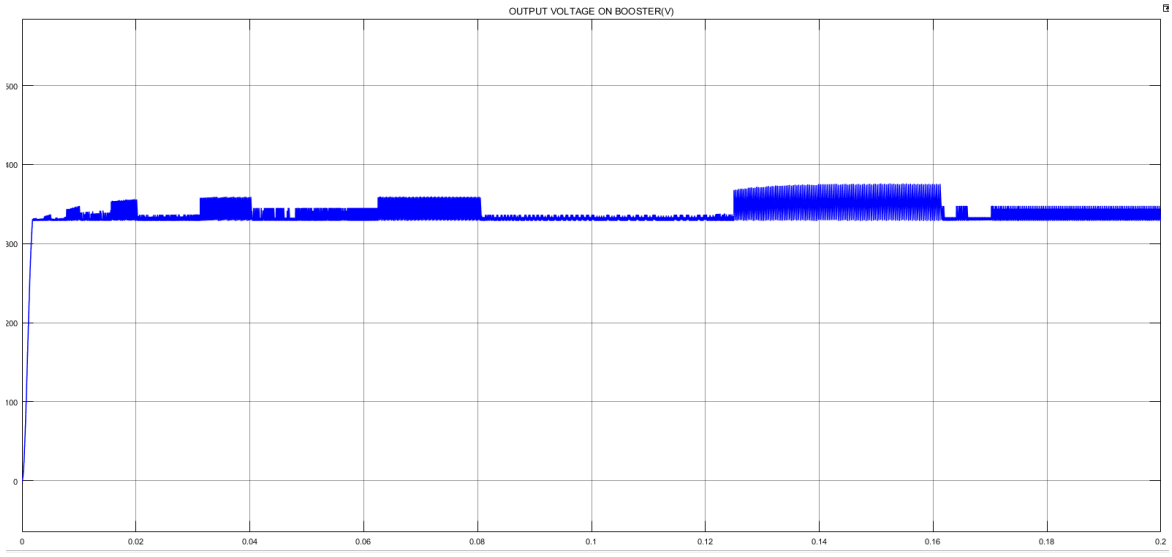

Figure 4. 9:Output voltage with control system

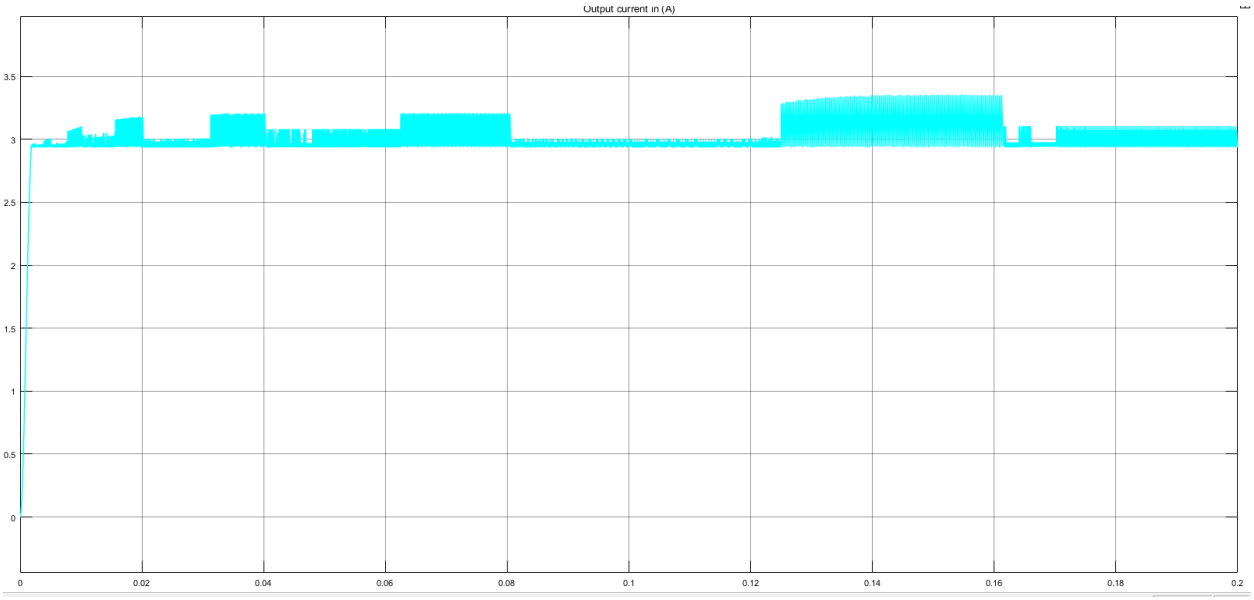

Figure 4. 10: Output current for closed loop converter

4.16. Design of PID-type Controllers

The majority of control systems in industry are based on the PID-type controllers. The name of PID refers to the fixed controller structure, which is formed from proportional, integral, and derivative term. In this project, the PI will be used to control the converter since the application of designed device is not in industrial areas. The standard PID controller can be written in parallel form:

$$C_{PID(s)} = \frac{U_s}{E_S} = K_p + \frac{K_I}{S} + \frac{K_D S}{\tau_d S + 1} \qquad (4.7)$$

A PID controller is the complete solution, including all terms. Tuning of PID controllers is difficult due to the need to determine four parameters

where U(s) and E(s) are the output and input of the PID controller respectively. The gains of the proportional, integral, and derivative terms are denoted as K_p, K_I , and K_D respectively. A first-order filter with the parameter τd is usually applied to the derivative term since the derivation is very sensitive to high-frequency noise. To design the PI controller let us consider: Voltage controller means outer loop and current controller means inner loop.

I. Voltage controller

Let us select the control time constant **Ts=200μs,Capacitor=5.7μF and the capacitor internal resistance Rc=4m ohm**

$K_p = \frac{C}{T} = 0.0285$ and $K_I = \frac{RC}{T} = 20$

II. Current controller

Let us select the control time constant **Ts=150μs,Inductor=4.5mH and the inductor internal resistance Rc=1m ohm**

$K_p = \frac{L}{T} = 29$ and $K_I = \frac{RL}{T} = 6.7$

4.4. Inverter simulation

The main function of the inverter in the solar PV system is to convert the DC voltage from DC-DC boost converter to alternating current (AC). The H-Bridge inverter consisting of four switched MOSFET was employed with two switches per leg as shown in Fig. 4.4. The switches are turned on and off diagonally with S1, S4 turning on the same time and then S2, S3 in succession.

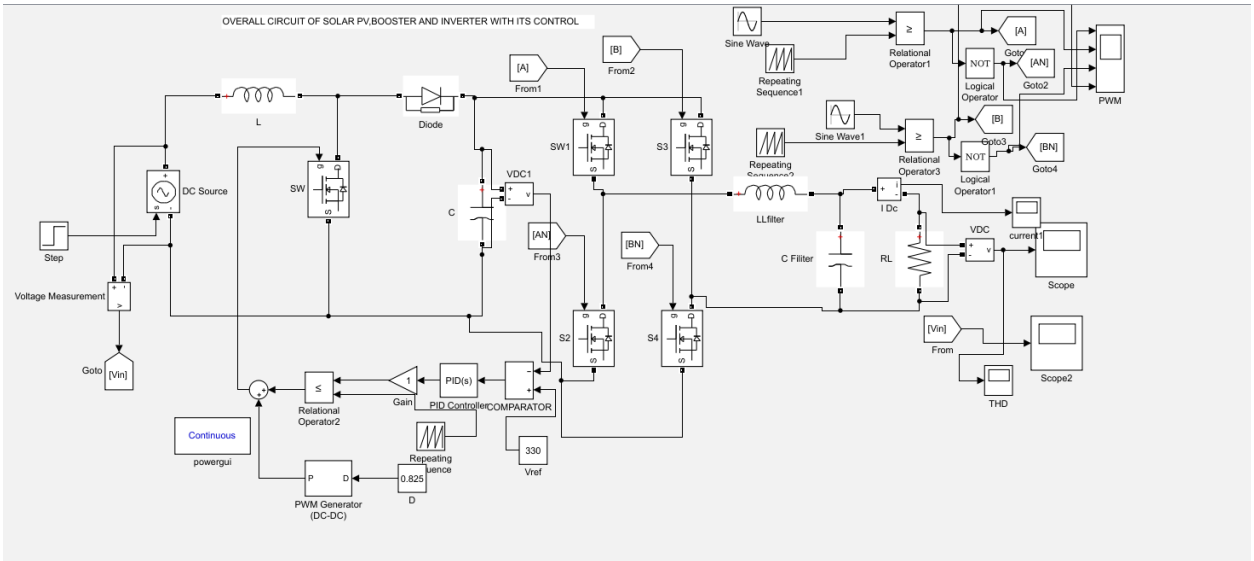

Figure 4. 11:Source , booster, Inverter, filter, and control

In a solar PV system, the inverter's main function is to convert DC power from the DC-DC boost converter to alternating current (AC). Using four switched MOSFETs with two switches per leg, an H-Bridge inverter design was used. This configuration (Fig. 4.11) is characterized by the diagonal activation of switches: S1 and S4 are activated simultaneously, while S2 and S3 are activated in turn. The simulation in the MATLAB/Simulink environment was carried out using the DC-DC boost converter design parameters that were input into the software, the input supply voltage is systematically adjusted in increments of 40 V and 60 V, ranging from 40 V to 60 V.

Table4. 1 The parameter used for designing the converter

Parameters	**Symbol**	**Values with its units**
Input voltage Range	Vin	40-60 V
Rated power	Po	1000 W
Nominal Voltage	Vn	48 V
Output voltage Peak	Vpeak	330 V
Output voltage RMS	V rms	230 v
Output current by average	Io	3A
Inductor ripple	ΔIo	0.625
Output voltage ripple	ΔVo	2V
Switching Frequency	fs	10000 Hz
Ripple current	I ripple	20%
Duty cycle	D	0.826
Inductor	L	0.653mH
Load(nonlinear)	RL	112 Ω

Output capacitor	C	22 µF

Figure 4:11 shows the complete Simulink model of the single-phase inverter with the closed-loop DC-DC converter. The MPPT regulates the variable supply voltage, which ranges from 40V to 60V. The DC-DC boost converters raise the variable supply voltage from the solar PV to a maximum of 330V. After then, the inverter transforms the controlled DC voltage into chopped AC voltage with a peak of 230V. The output is then sent through an LC low-pass filter to create a voltage and current output that are both pure sinusoidal AC as shown in figure 4.15

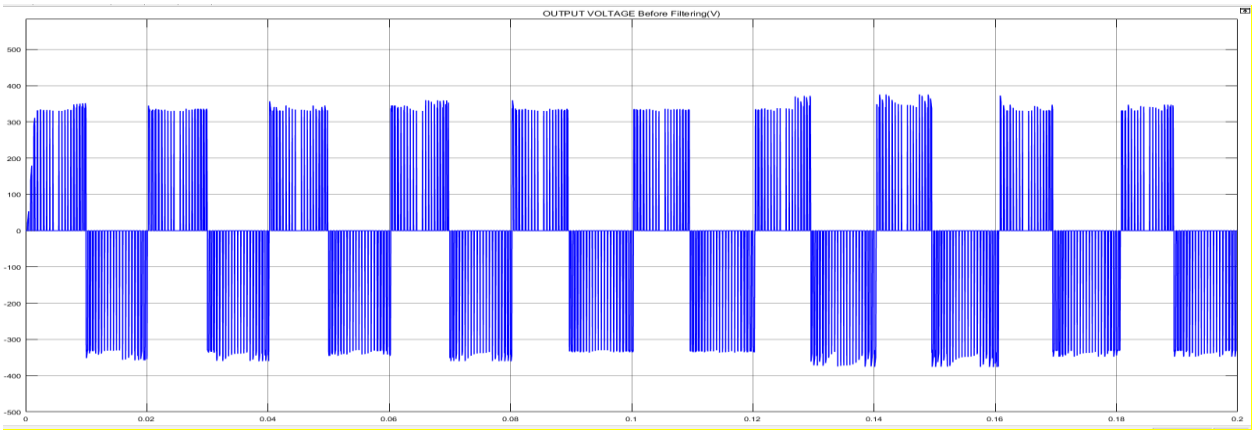

Figure 4. 12: DC-AC converter output voltage before filtering

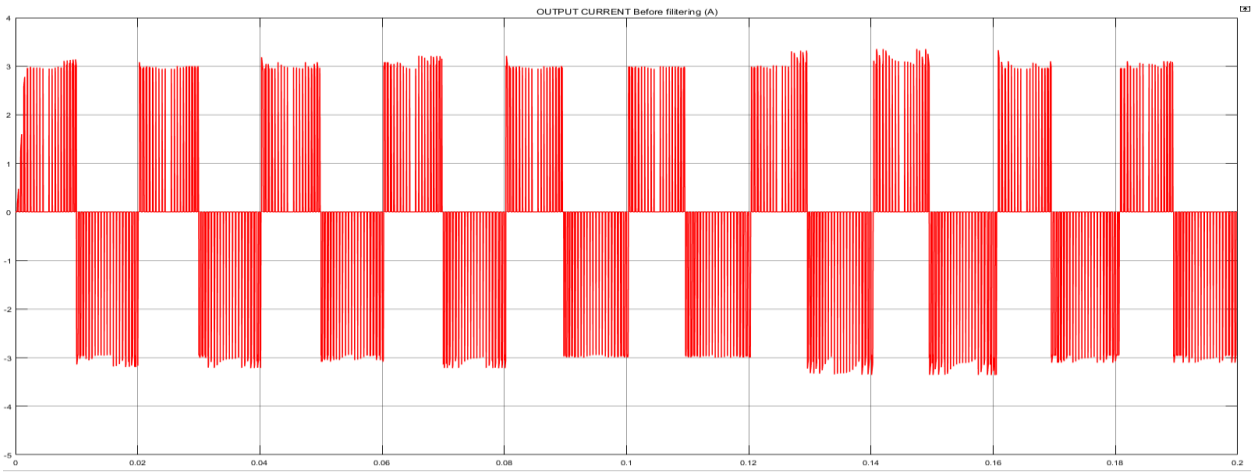

Figure 4. 13: DC-AC converter output voltage before filtering

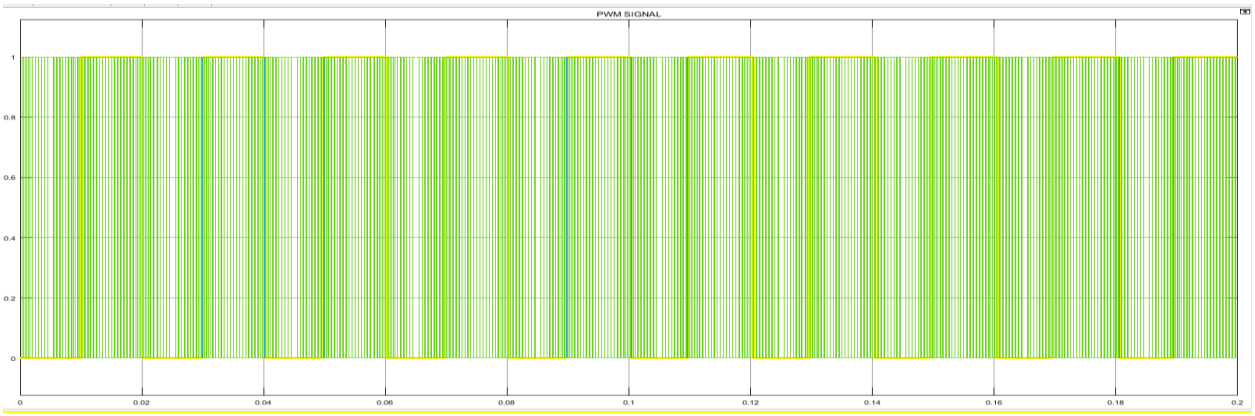

Figure 4. 14: Signal pulse to trigger the inverter.

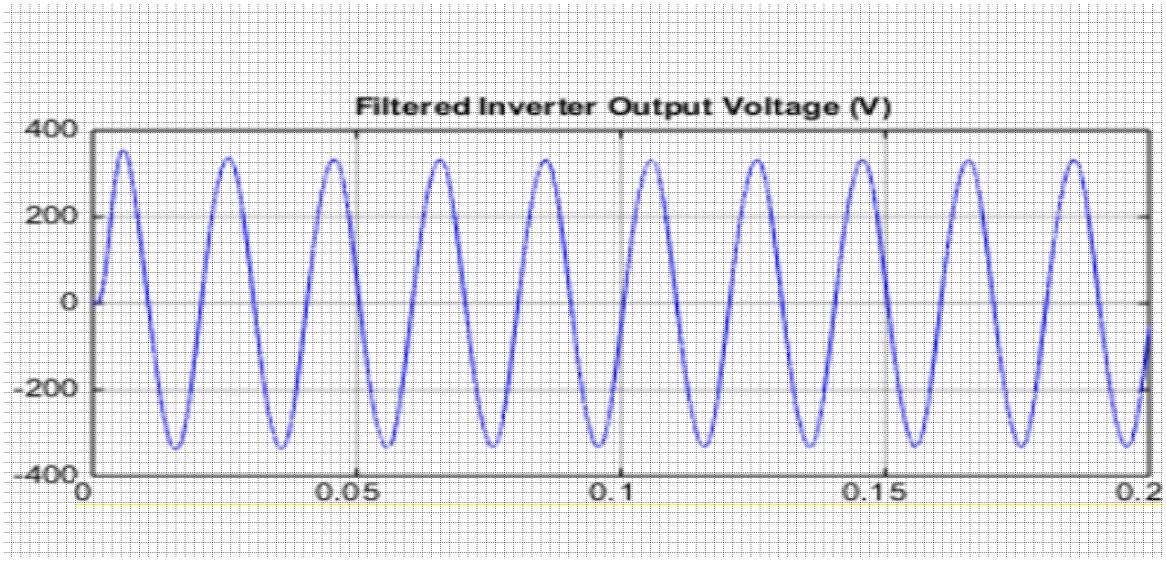

Figure 4. 15: Output voltage (rms values)

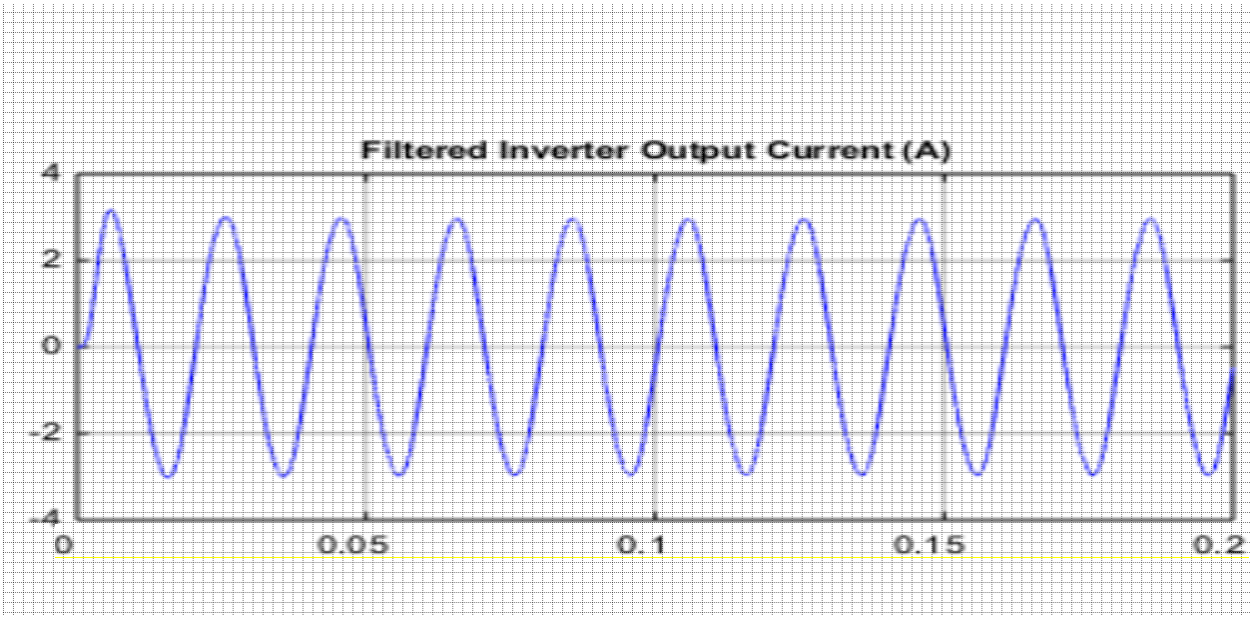

Figure 4. 16: current (rms values)

4.5 Discussion for results

The input voltage needs a boost converter up to 330V peak. The output voltage is purely AC Voltage with Magnitude around 230Vrms with index modulation of one as shown on Fig 4.15, the filter provides smooth AC signal after removing ripples. Using sinusoidal pulse width modulation control, the inverter switches are managed. Practically speaking, inverters usually produce non-sinusoidal waveforms with certain harmonics. By using low pass filter, harmonics are eliminated. SIC MOSFEET have been selected for our simulation due to Today, technology allows the use of extremely fast switching components with the ability to withstand high currents and voltages. The source selected from SIMULINK environment to easy simulation and provide accurate results. In case the solar is not available the battery provides the supply to the inverter (it starts to be discharged as show on figure 4.9

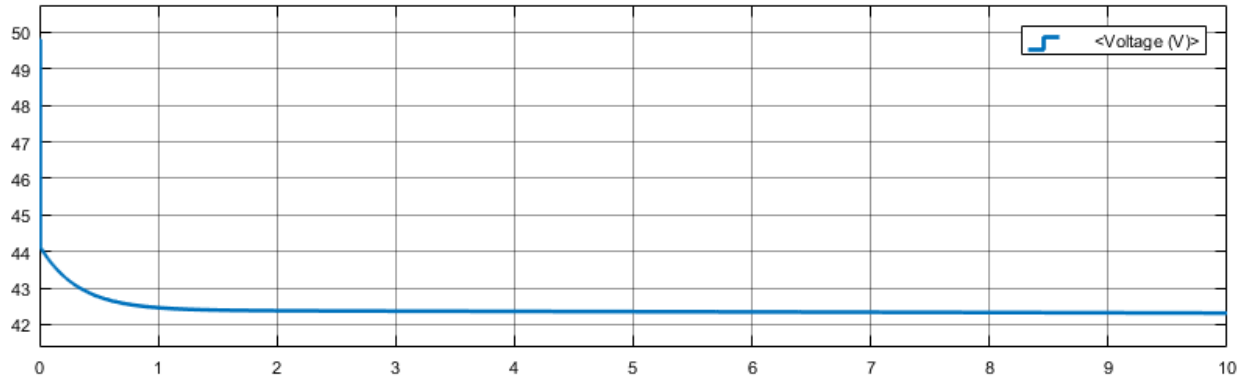

Figure 4. 17: Battery voltage during discharging

The voltage from PV keep supplying the system depending on the solar radiation. for constant irradiation the voltage obtained 48 v is shown on the figure 4.10

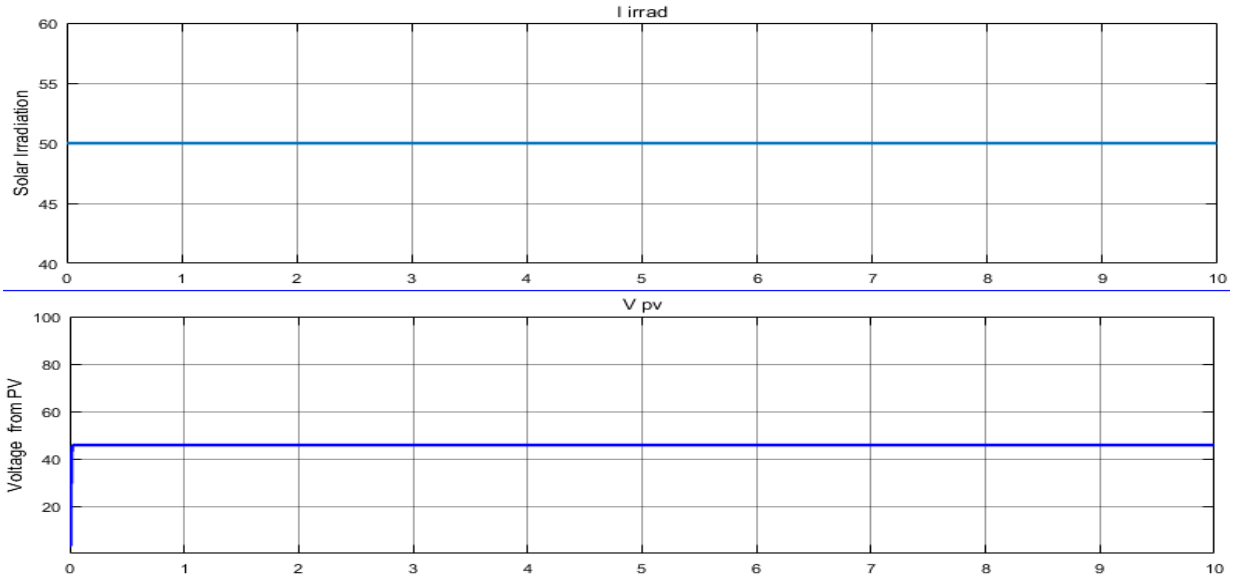

Figure 4. 18: Voltage from PV at constant Irradiation

To maximize the use of solar energy, it is helpful to focus on improving solar cell efficiency via advances in manufacturing methods. Furthermore, to adapt solar PV generation to applications in both small- and large-scale power systems, it is imperative to investigate advancements in power electronic equipment. Also, to increase the voltage and the current for the solar PV the number of modules can connected in series and parallel as depicted by figure4.11 below respectively

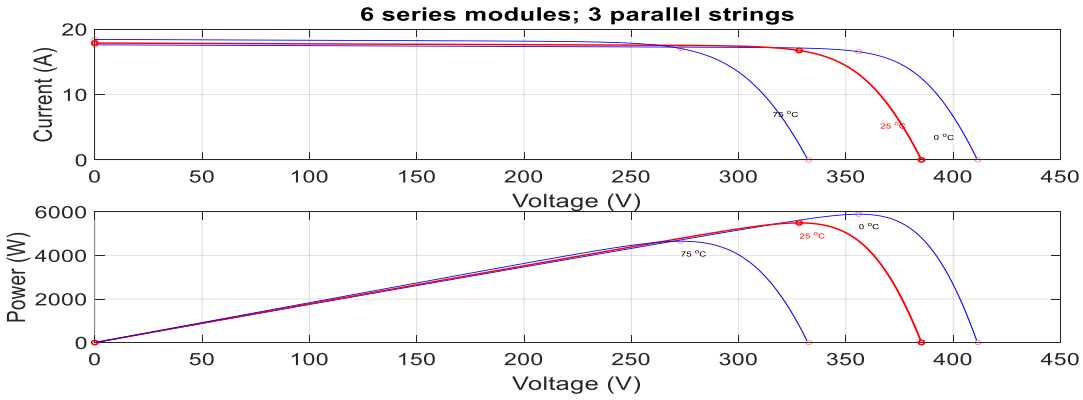

Figure 4. 19:6 Series modules and 3 parallel strings

Six modules are connected in series in this configuration, meaning that the positive terminal of one module is connected to the next module's negative terminal. This increases the cumulative voltage throughout the series. Three sets of these parallel-arranged series-connected modules are also present. It is possible to carry more current with this parallel configuration. Temperature variations have a significant impact on how well solar PV module's function. Variations in temperature may influence the solar panels' output and efficiency. The efficiency of the solar cells may decline with temperature, which could result in a drop-in power output. On the other hand, lower temperatures can increase solar panel efficiency. A balance between voltage and current is made possible by designing the configuration with both series and parallel connections, which maximizes the system's efficiency across a variety of environmental conditions, including temperature variations.

CHAPITER 5: DESING AND SIMULATION OF INVERTER UNDER LINEAR AND NON-LINEAR LOAD

5.1. Introduction

The inverter takes input from diverse DC sources such as batteries, photovoltaic cells, fuel cells, alternators, and more. Single-phase inverter circuits typically utilize two configurations: half-bridge and full bridge. This design specifically concentrates on the full bridge configuration. Inverters find extensive applications, ranging from small, switched power supplies for computers to large-scale electric utility applications for transporting bulk power.

5.2. Single-Phase Standalone Inverter Model and Control

The physical structure of the standalone single-phase inverter under consideration in this thesis is shown in **Fig. 5:1**. The inverter supplies a standalone load through an LC filter, which consists of a L_f with parasite resistance, R_f, and the capacitor C_f. The low-pass filter components have the most influence on the filter's dynamics. Furthermore, the dynamics of the DC-power port are omitted in the following analysis because the DC-voltage is controlled by the storage battery's back-boost converter. The control system is implemented as a cascaded loop, with the current and voltage loops working in tandem. The current control loop oversees controlling the current through the inductor filter and providing overcurrent protection, whereas the voltage control loop oversees regulating the load voltage and generating the reference current. Furthermore, the voltage loop provides harmonics support function under non-linear load, moreover those are loops stabilized by proportional integral and derivative (PID).

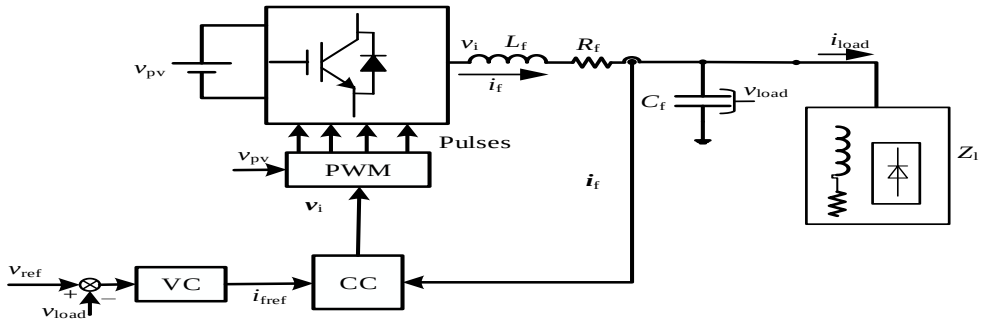

Figure 5. 1:Structure of the VSC

5.3. Dynamic Model of the Inverter Power Circuit

From **Fig. 5:1**, the power circuit consists of C_f, L_f, and Z_l. By applying the Kirchhoff voltage law, the mathematical equations describing the dynamics of the power part of the inverter can be obtained as **in Eq. 5. 8, Eq. 5. 9 and Eq. 5. 10** for C_f, L_f, and L_g, respectively, in the dq-reference frame.

$$C_f \frac{dv_{load}}{dt} = i_f - i_{load} \tag{5.1}$$

$$L_f \frac{di_f}{dt} = v_i - R_f i_f + v_{load} \tag{5.2}$$

where v_i and v_{load} are the converter and load voltage, respectively, if and i_{load}, are the filter current and load current, respectively. The output current could be expressed as follows:

$$i_{load} = \frac{v_{load}}{Z_{load}} \tag{5.3}$$

Z_{load}, can be a linear load or a non-linear load and the inverter is responsible for providing the required output voltage.

5.4 Design of each component for Filter

First-order L-filter, second-order LC-filter, and third order LCL-filter are the three main inverter harmonic filter topologies. The inverter switching components are only somewhat attenuated by the L-filter; therefore, an extra shunt element (the LC-filter) is required to further lower the switching frequency components. For the shunt component to remain low reactance at the switching frequency, careful selection is required.

It should also have high impedance in the control frequency band, which is usually accomplished by using a capacitor as the shunt element. A single-ended LC filter's cutoff or resonant frequency is established by[41].

$$\mathbf{F_0} = \frac{\mathbf{1}}{\mathbf{2\pi\sqrt{LC}}} \tag{5.5}$$

Where Fo is cutoff frequency

Resonance in the AC output voltage and a time delay are caused by the PWM inverter controlling the output voltage on the LC filter capacitor. A low pass filter made from an inductor and a capacitor is shown in Figure 5:3. The inductor and capacitor values are taken into consideration in the filter design. A clean sinusoidal AC output at 50 Hz can be achieved by simulating the application of a passive LC low pass filter. The low pass filter's cutoff frequency,C_f, is purposefully chosen to be less than 1/25th of the inverter switching frequency.

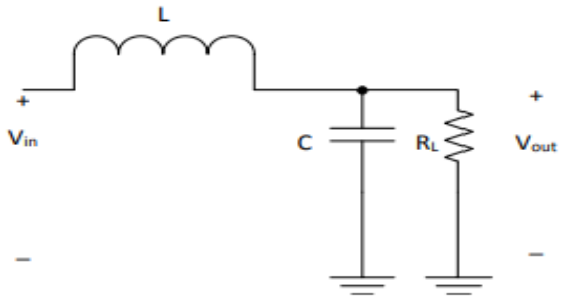

Figure5. 2:LC low pass Filter [74]

From equation (12), The value of inductor and capacitor can be calculated as

$$L=\frac{R_L\times\sqrt{2}}{\omega_0} \tag{5.6}$$

To make sure that the voltage drop across the inductor stays below 5% of the inverter output RMS voltage, the filter inductor's value ($L\ filter$) is calculated.

$$I_{Lmax} \times 2\pi f L_{Filter} \leq 0.005 V_{rms} \tag{5.7}$$

$I_{Lmax:}$ Maximum RMS load current, V_{rms}: Inverter RMS output voltage RMS and f: Output voltage frequency.

$$C=\frac{1}{\omega_0\times R_L\times\sqrt{2}} \tag{5.8}$$

Where C capacitor, L inductor and RL Load Resistor. Sources like[41]offer a methodical approach to LC filter design. During the design process, several factors need to be taken into account, such as current ripple, filter size, and attenuation of switching ripple.

The LC filter may cause resonance because of the inductor's intrinsically low parasitic resistance; the resonance frequency may change depending on the applied load. As a result, passive or active dampening must be included. This is done by attaching a resistor to the capacitor or inductor filter. The rated active power, switching, DC-port voltage, output voltage, and output RMS voltage are the parameters for the LC filter. The base capacitance and base impedance are defined by the following formulae.

$$Z_b = \frac{V_{load}}{P_n} \tag{5.9}$$

$$C_b = \frac{1}{\omega_b Z_b} \tag{5.10}$$

Where P_n is nominal power

The evaluation of the filter components is conducted in the following manner, beginning with the reference values: The highest power factor variation that the load experiences must not exceed 5% to compute the filter capacitance. As a result, the filter capacitance may be calculated as follows:

$$C_f = 0.05 C_b \tag{5.11}$$

The filter inductor is sized based on the acceptable maximum peak to peak current ripples, which can be express:

$$\Delta i_f = \frac{V_{pv}}{2 L_f f_s} \tag{5.12}$$

Where f_s is switching frequency

Considering the values of filter inductor and filter capacitor, the designed values must agree with the following condition.

$$10 f_o < f_{res} < f_s \tag{5.13}$$

5.5. Open loop dynamics for inverter

By performing the linearization and transform the equation [5.0] to [5.13] into Laplace transform, the open loop transfer function can be obtained as:

$$(L_f s + R_f) i_f = V_{in} - V_{load} \tag{5.14}$$

$$(C_f s) V_{load} = i_f - \frac{V_{load}}{Z_{load}} \tag{5.15}$$

Combining the above 2 equations,

$$V_{in} = ((L_f s + R_f) * \frac{(Z_{load} * (C_f s) + 1)}{Z_{load}} + 1) V_{load} \quad (5.16)$$

$$\frac{V_{load}}{V_{in}} = G_{open} = \frac{1}{((L_f s + R_f) * \frac{(Z_{load} * C_f s + 1)}{Z_{load}} + 1)} \quad (5.17)$$

By analyzing the above transfer function under variation of the system parameters,

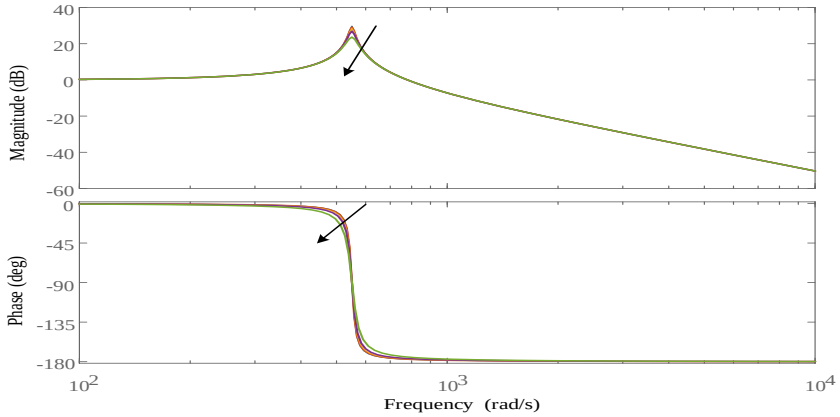

Figure5. 3:impact of resistive load on inverter dynamics

An elevated-frequency LC resonance manifests in the open-loop gain at 160Hz, exhibiting a considerably high resonant amplitude and a pronounced phase shift passing through −180◦.

This invariably and unequivocally results in instability in the closed-loop system for all current controller gains, coupled with a sluggish dynamic response. Consequently, even with the inclusion of physical internal damping terms for the output filter, damping solutions become imperative in this scenario to constrain the elevated gain at the LCL resonance frequency for the stability of the closed-loop control system. The inductors are designed to filter out high frequencies, and the capacitors perform a similar function, allowing only low-frequency signals to reach the load. The incorporation of capacitors and inductors in a circuit is likely to induce resonant effects at a specific frequency, and the arrow denotes the variation in load resistance.

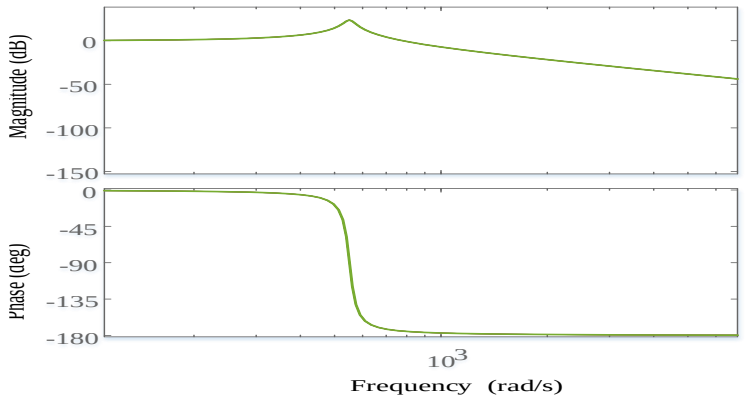

Figure5. 4:Effects of inductive load on LC filter resonance

As the frequency increases, the capacitor's impedance decreases. Due to the low impedance running in parallel with the load resistance, high-frequency signals tend to be short-circuited, causing most of the voltage to drop across the series resistor. The dynamics of the load do not impact the resonance effect of the filter. A low-pass filter facilitates the smooth passage of low-frequency signals from the source to the load while impeding the transmission of high-frequency signals. Inductive low-pass filters incorporate an inductor connected to the load, whereas capacitive low-pass filters involve connecting a resistor in series and a capacitor in parallel to the load. The former aims to "block" undesirable frequency signals, while the latter aims to filter them out. The cutoff frequency for a low-pass filter is the frequency at which the output (load) voltage reaches 70.7% of the input (source) voltage. Beyond the cutoff frequency, the output voltage falls below 70.7% of the input, and vice versa.

As the resistance increases, the filter becomes under damped, and the resistor becomes too small. A large transient oscillation in the LC circuit can be dampened by connecting a resistance to the LC circuit. Active damping is commonly used to dampen the inverter system's resonance behavior, thereby stabilizing the system. By applying the active damping using filter inductor current, the equation in 5.15 become:

$$(L_f s + R_f) i_f = V_{in} - s C_f K_d - V_{load}) \tag{5.18}$$

Performing the same manipulation as above, the impact of damping effect can be observed.

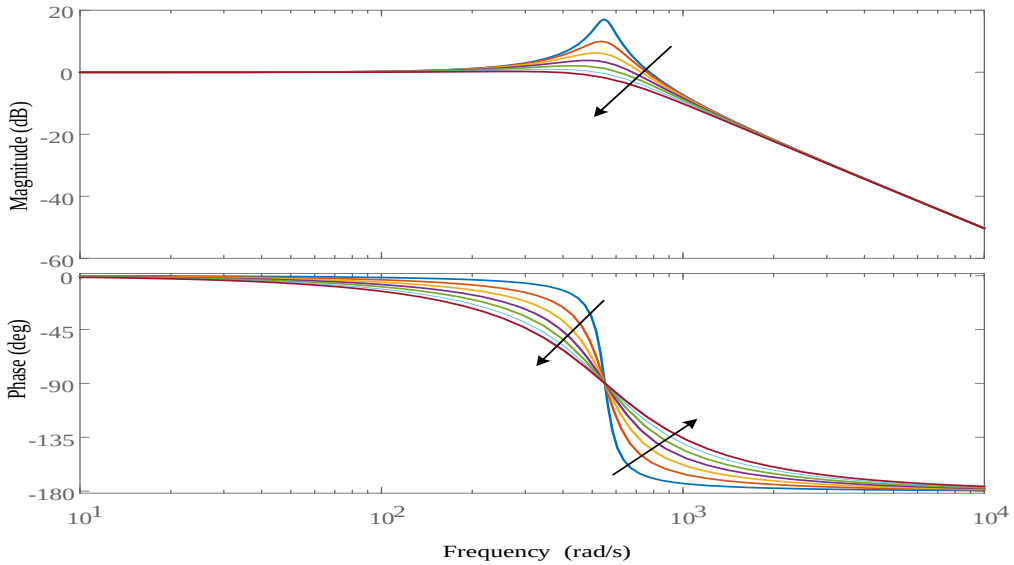

Figure5. 5:Impact of damping constant on inverter dynamics

The LC resonance peak is gradually damped as the feedback gain increases, while the resonant frequency is slightly increased. When damping is used, the overall bandwidth of the control system increases, resulting in a faster time response. By increasing the damping coefficient, the dynamics of the LC filter are improved.

5.6. Designing the control loops.

To provide high-quality power, voltage and current must be dynamically and precisely controlled. To achieve the inverter voltage regulation, it is necessary to design cascaded control loops that enhance the stable operation of the inverter system. The inner current loop will be responsible for current flowing through the filter inductor control and provide current protection functionality.

It is in nature designed to faster than the outer voltage loop and slower than the switching frequency [76] The outer voltage loop regulate the load voltage to follow the reference voltage. In addition, it is also designed to provide harmonics support functionality.

Among different controller design methods used in power system, Internal Mode Control (IMC) design method is selected due to its benefits such as, faster step response, less overshoot in the transient, higher axes decoupling; and more robustness against fault and Response compared to others.

5.6.1. Internal Mode Control

Internal model control (IMC) is an alternative to conventional feedback control and has a long history in the process industry. In fact, IMC has found many applications in electrical power systems, such as load frequency control, the control of DC/DC converters, and electric drivers. IMC is based on the internal model principle, which states that: Control can be achieved only if the control system encapsulates, either implicitly or explicitly, some representation of the process to be controlled. The structure of IMC can be observed in the fig. below. The transfer

$G_p(s), G_c(s)$ and $\widetilde{G_p}(s)$ are process controller and model of the process, respectively.

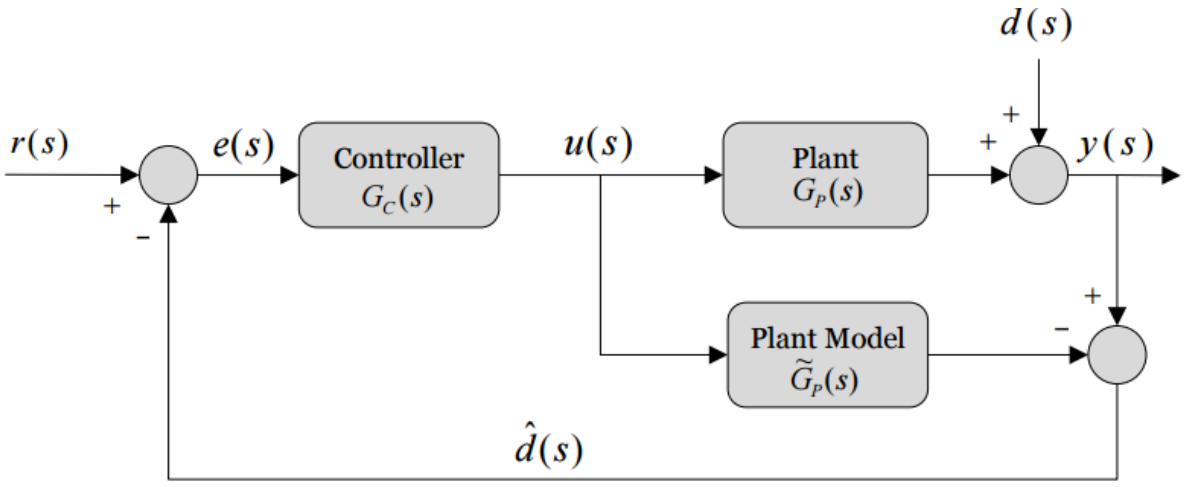

Figure5. 6:Control System for internal model control

From the Figure 5.7 above, the standard feedback form of the IMC controller K(s) can be deduced as

$$K(s) = \frac{G_C(s)}{1-G_C(s)\widetilde{G_p}(s)'} \qquad 5.19$$

To make $G_C(s)$ proper, the plant model is cascaded with the low pass filter and can be expressed as

$$G_C(s) = \widetilde{G_p}(s)^{-1} * \frac{1}{(\lambda s+1)^n} \qquad 5.20$$

where λ is the tuning parameter and n is an integer, which will be equal to the order of the numerator plus 1.

5.6.2. Inner current loop

In the given scenario, following the IMC approach described above, an inner current loop controller is designed. Through the transfer function G_i, the filter inductor current, represented as i_f, is connected to the input voltage Vin:

$$\frac{i_f}{Vin} = G_i = \frac{1}{L_f s + R_f} \tag{5.21}$$

In this case, s stands for the Laplace variable, R_f for the filter resistance, and R_f for the filter inductance. This theory establishes the criteria for choosing the controller bandwidth and uses the transfer function G_i to represent the plant. To properly counteract the dynamics produced by the switching frequency, the switching frequency needs to be 10 times larger than the bandwidth of the inner current controller. The current controller is obtained as:

$$\mathrm{K_c} = \frac{L_f s + R_f}{s\lambda} \tag{5.22}$$

Which can be converted easily into its equivalent PID controller, with proportional constant

$$K_p = \frac{L_f}{\lambda} \text{ and } K_i = \frac{R_f}{\lambda} \tag{5.23}$$

To summarize, the inner current loop theory relies on the IMC approach and makes use of the transfer function G_i, which is obtained from the filter inductor current. To properly eliminate the switching frequency dynamics, the switching frequency must be 10 times higher than the inner current controller bandwidth.

This means that the controller bandwidth is very important. The overall form of the current controller is described, and for practical implementation, it may be easily turned into a PID controller, where the proportional and integral components of the controller are determined by K_p and K_i.

5.6.3. Outer loop controller design.

By considering the inner current loop dynamics, and the dynamics of filter capacitor, while neglecting the load impact, the closed loop voltage control loop can be observed in figure below: In the designed system aimed at canceling load harmonics, a resonance controller for the inverter is introduced. Initially, the Internal Model Control (IMC) is applied to shape the outer loop

controller, and the resonance terms are cascaded to it to counteract load nonlinearity effects. When load effects are disregarded, the expression for G_{out} simplifies to: Here, G_v is tuned using IMC, and the theory described earlier is applied, considering the plant as $G_c \frac{1}{sC_f}$

The resonance terms are subsequently designed by examining the impact of the integrator term on the Bode plot of the voltage open-loop plant, which is expressed as:

$$G_{out} = G_v * G_c * \frac{1}{sC_f + 1/Z_l} \tag{5.24}$$

This approach allows for the systematic inclusion of resonance controllers in the inverter system, contributing to improved performance and the cancellation of undesirable load harmonics.

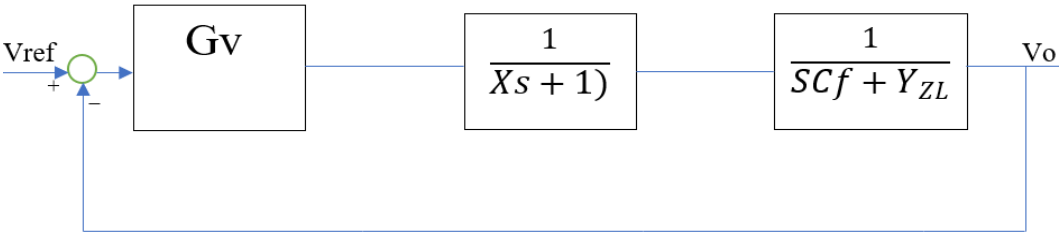

Figure5. 7:Overall Control system of the plant

This approach allows for the systematic inclusion of resonance controllers in the inverter system, contributing to improved performance and the cancellation of undesirable load harmonics.

$$\text{Gv} = C_f \frac{((\lambda_s+1)}{\lambda_o{}^2 S+2\lambda_o} + \frac{K_2\, S}{S^2+\omega_o{}^2} + \frac{K_2\, S}{S^2+(3\omega_o)^2} + \sum_{k=5,7,11}^{1} K = \frac{K_n\, S}{S^2+(n\omega_o)^2} \tag{5-25}$$

$$G_{out} = G_v * G_c * \frac{1}{sC_f + \frac{1}{Z_l}} \tag{5-26}$$

Current loop

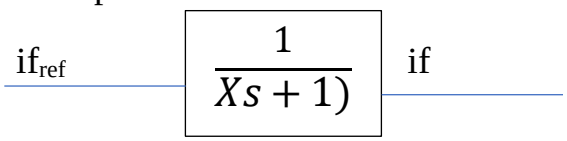

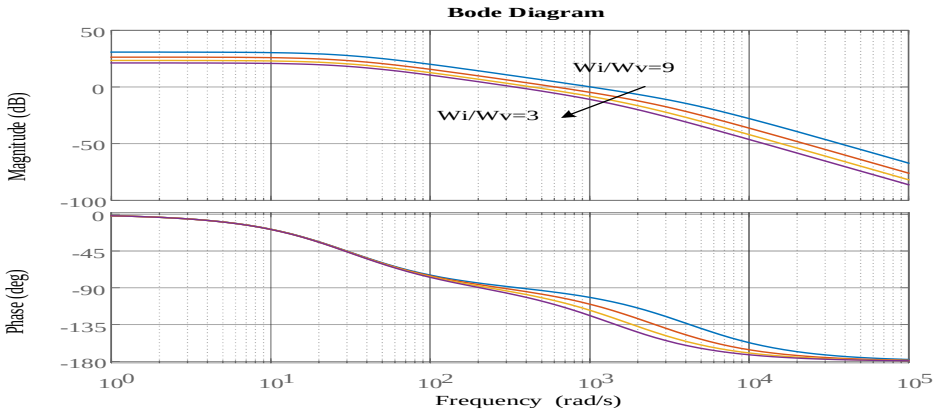

Figure5. 8:Impact ratio of outer and inner loop bandwidth

Figure 5.8 stands for the impact ratio between the inner and outer loop bandwidths in the context of a control system is shown in the figure. The system's gain margin is clearly affected by a drop in the outer loop bandwidth. The outer loop, which usually includes more control features, has a narrower bandwidth.

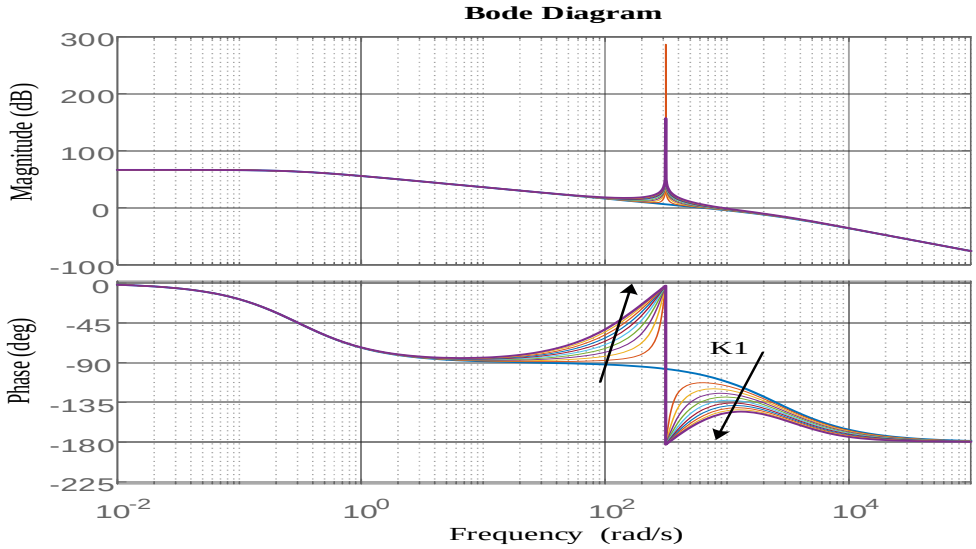

Figure5. 9:Impact of resonant controller at nominal frequency

The system's gain margin rises because of this bandwidth reduction. One key indicator of a control system's stability and resilience is its gain margin. Intentionally reducing the outer loop bandwidth leads to a more conservative control method that prioritizes stability over quick response to changes.

The higher gain margin, which reflects this adjustment, suggests that the system becomes more resilient to changes and disruptions. To sum up, the graphic illustrates how the inner and outer loop bandwidths interact, showing how the gain margin rises with decreasing outer loop bandwidth. This knowledge is helpful when fine-tuning control systems to strike the right balance between performance and stability, especially in applications where robustness is a top concern. Moreover, the outer loop is designed to be slow enough at least 1/3 of the inner current loop to cancel the loop interaction.

The figure 5.9 that the sentence alludes to is probably a Bode diagram that shows the effect of a resonant controller at the nominal frequency. A Bode diagram provides a visual representation of a system's frequency response, making it possible to observe the system's behavior at various frequencies. An important point of interest is the nominal frequency, which is frequently connected to the system's intended operating frequency. The response of the system at the nominal frequency is influenced by the resonant controller, as shown in the figure.

The cutoff frequency, which indicates the frequency at which the system's reaction begins to weaken, is one factor to consider. This cutoff frequency is important since it establishes the system's bandwidth. Furthermore, the word "spikes" implies that the graphic might have Bode diagram resonances or peaks. The resonant controller seeks to control or improve this behavior at nominal frequency. These spikes may indicate resonant behaviors at frequencies. In its simplest form, the figure illustrates how a resonant controller affects the frequency response of the system at the nominal frequency. It highlights the cutoff frequency and any spikes present, offering valuable information on how the controller affects system dynamics and resonant properties.

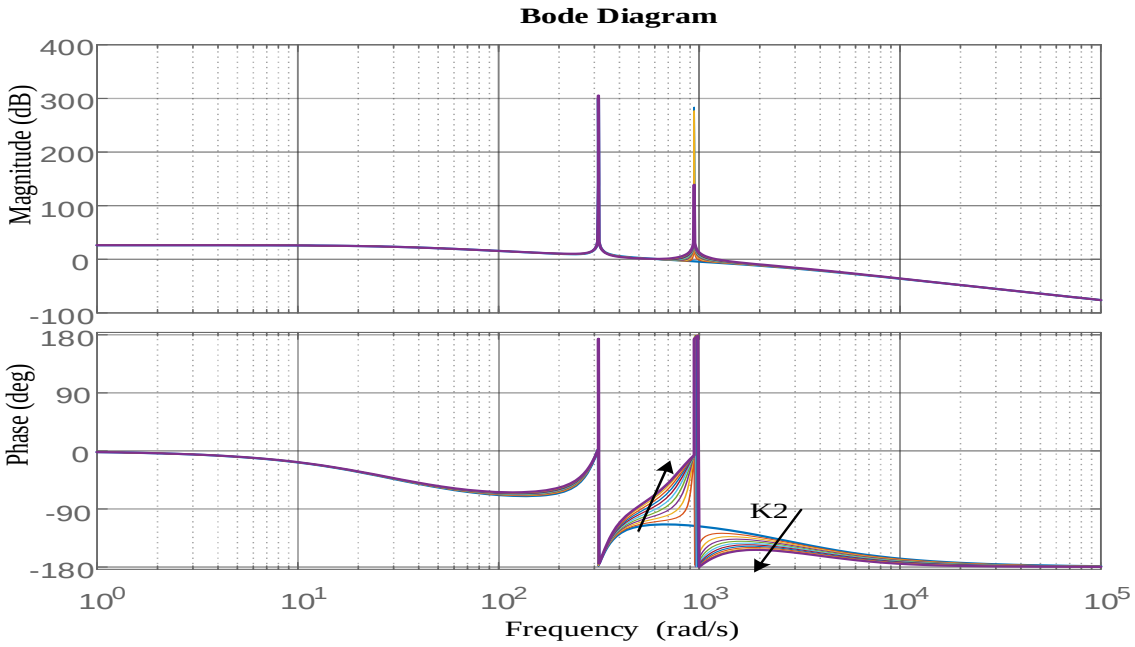

Figure 5. 10:Impact of resonance term at 3rd harmonic

From above figure describes the Bode diagram which shows how the resonance term at the third harmonic affects the frequency response of the system. Peaks or spikes become more noticeable at the third harmonic, suggesting resonant behaviors at this frequency. These spikes exhibit a 180-degree phase shift and a discernible rise in magnitude on the Bode chart. The signal strength reaching 300 dB indicates a very high gain at the third harmonic, indicating a significant resonance effect. A resonance phenomenon where the system is highly sensitive to the third harmonic frequency is shown by a prominent peak in the magnitude response.

Notable is the phase shift at the third harmonic, which reaches 180 degrees. A 180-degree phase shift indicates that the signal is inverted, indicating that the response of the system is out of phase with the input signal at this frequency. To sum up, the resonance term at the third harmonic causes spikes in the Bode diagram that have a 180-degree phase shift and a magnitude of up to 300 dB. These findings demonstrate the system's sensitivity and behaviors at this specific frequency by pointing to a notable resonant response at the third harmonics.

5.7. Simulation results in PLECS

This full-bridge voltage source inverter is fed from a DC source such that the fundamental RMS output voltage is approximately 220V. The desired fundamental frequency is 50 Hz. To verify the results also the simulation model has simulated in PLECS as shown below in Figure 5.12.

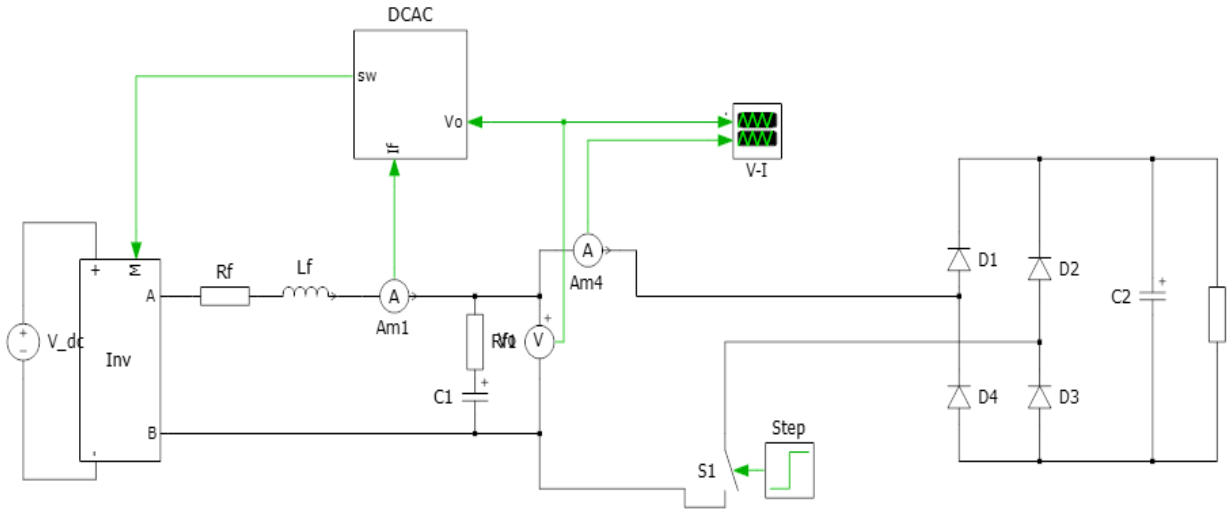

Figure5. 11:Complete piecewise linear electrical circuit Simulation for stability analysis

Essential elements are included in a PLECS model for a DC to AC inverter system in order to replicate a realistic and dynamic electrical environment. A smoothing capacitor, which is essential for voltage stability, an inverter converter (which converts DC to AC), filters (Rf, Lf) to mimic harmonic filtering and smoothing of the AC output, a nonlinear load element that mimics real-world nonlinear characteristics, and a resistive load component that mimics resistive behaviors in the inverter output are all included in the model. In the simulations, the DC terminal voltage has been considered constant as it was regulated by the battery charging-discharging controller.

5.7.1. Case 1. Simulation results with linear load

The load voltage and current when there is an increase in load current from 1.5 A to 3.85 A respectively, can be observed in Figure 4.13. As can be observed, when the load change, the load current change respectively. It can be noted that even though the load changed, the terminal voltage remains unaffected.

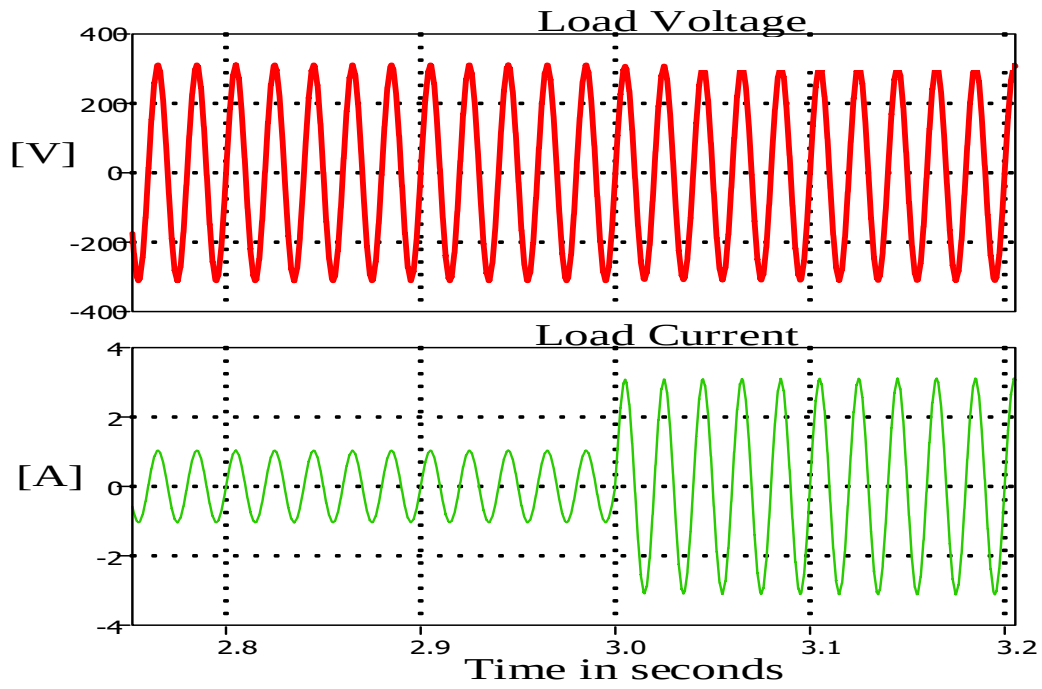

Figure5. 12:Output voltage and current for linear load changing from 200 to 15 Ω

The load decreased at the 3 seconds which made the current to increase until 3.5A which means that the controller tried to keep the voltage to stay in acceptable range as it is required by the IEEE standard 1547 published in 2018.

5.7.2. Case 2. Simulation results with nonlinear load

Non-linear loads introduce harmonics which can cause voltage distortion and affect the performance of other connected equipment. Load modelling involves determining the harmonic content of the load, including the magnitude and phase angle of each harmonic component. The load voltage and current when there is an increase in load current up to 15A, can be observed in Figure 5.14. As can be observed, when the load changes, the load current significantly increases respectively. It can be noted that even though the load and current changed, the terminal voltage remains unaffected

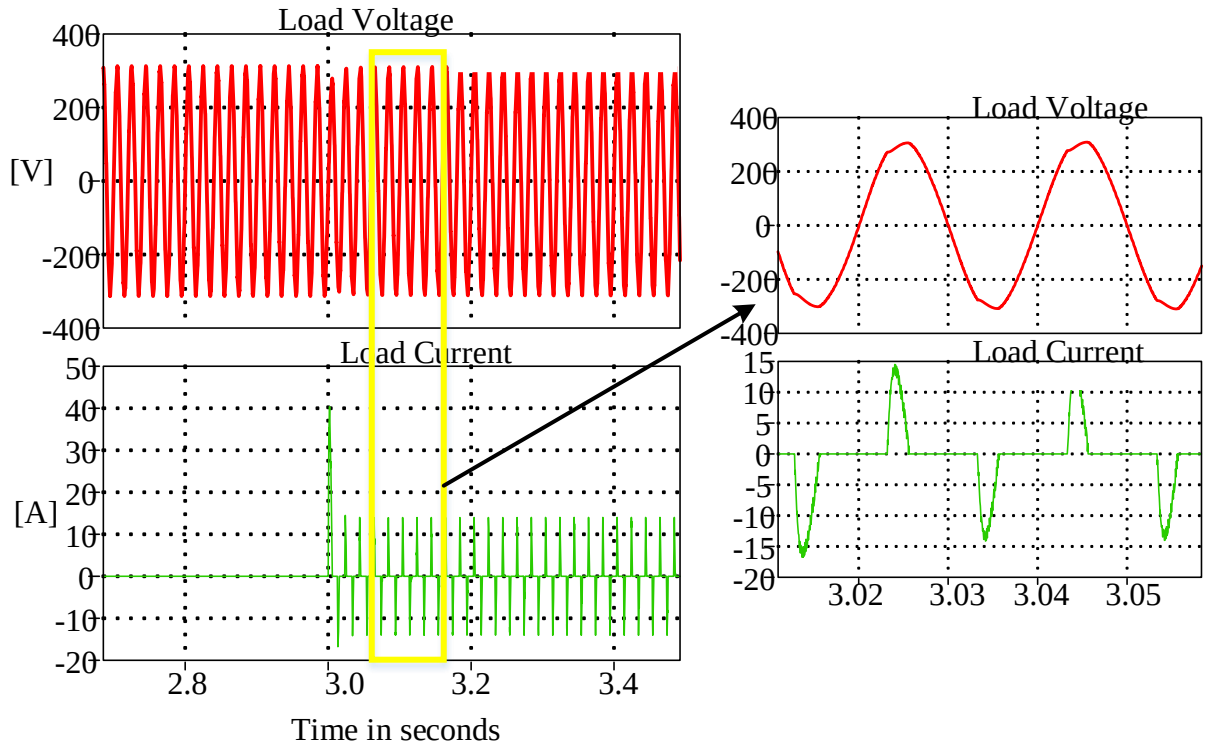

Figure5. 13: Output voltage and current for nonlinear load from 0 to 150 Ω

Figure 5.13 illustrates how a nonlinear load affects the stability of the system. The current has demonstrated a significant increase, fluctuating dynamically over time. The nonlinear load's current are depicted in the picture as it changes from 0 to 15 A, giving an idea of how the electrical properties are evolving. The observed drop in rise in current demonstrate the difficulties caused by nonlinearities and how they can jeopardize system stability. This dynamic response, shown the necessity for careful evaluation and mitigation techniques to ensure system stability under variable load conditions.

CHAPITER 6: CONCLUSION, FUTURE WORK AND RECOMMENDATIONS

6.1 Recommendations

As the modern Technology for today is increasing, it is advised to investigate sophisticated control algorithms for better reaction and stability in order to improve the design of residential DC to AC converters. Examining how energy storage devices, such batteries, might be integrated to improve energy efficiency and offer backup power in the event of a grid failure.

More sustainable and ecologically friendly household energy systems can be created by considering the effects of renewable energy sources, such as solar panels, in addition to the converter. For these systems to be more widely adopted in homes, ongoing research and development efforts should concentrate on reducing converter size, weight, and cost while optimizing efficiency. This means that electronic devices based on silicon carbide (SiC) can operate faster and with less energy loss, improving overall efficiency.

6.2 Conclusion

Improving the efficiency and dependability of domestic power systems requires careful consideration of the best design and simulation of a home DC to AC converter. The developed converter may effectively suit the specific requirements of household applications by carefully considering critical characteristics including architecture, control techniques, and component selection Also efficient power converter connects the solar energy generator to the loads and delivers the generated energy to different converter and loads. Electronic power converters are used to improve power quality because solar PV systems are inherently intermittent and constantly fluctuate. The simulation results show how the converter performs in various situations and offer important information on how it behaves and works in the MATLAB/Simulink environment. A single-phase inverter and a DC-DC boost converter are used in the design and modelling to accommodate a solar PV system with a wide input voltage range. According to the results of the simulation, the DC-DC boost converter successfully controlled the varied supply DC input voltage, which came from the solar PV and ranged from 40V to 60V. It also kept the voltage constant at 330V DC, even when the supply voltage fluctuated.

The bridge inverter successfully converts the DC voltage to 330 V peak AC voltage and the inverter output voltage has 230V rms AC value which can make the system to supply AC local load as well as grid. This study advances home power systems by providing a solution that strikes a balance between sustainability, affordability, and performance.

6.3 Future Work

To facilitate effective coordination between residential energy systems and the larger electrical grid, future research in this field should focus on the integration of smart grid technologies and sophisticated communication protocols. The performance of the converter could be further optimized by investigating the possibilities of machine learning algorithms for adaptive control techniques based on demand patterns seen in real time. Furthermore, examining the effects of cutting-edge technology like wide-bandgap semiconductors may improve converter design, leading in increased efficiency and lower losses. Future research into the integration of energy storage technologies with DC to AC converters is an intriguing prospect for improving the resilience, efficiency, and sustainability of residential energy systems.

6.Referances.

[1] S. Bhutada and S. R. Nigam, "Single Phase PV Inverter Applying a Dual Boost Technology," *Int. J. Appl. Power Eng.*, vol. 5, no. 2, p. 95, 2016, doi: 10.11591/ijape.v5.i2.pp95-102.

[2] S. Shafiee and E. T. Ã, "When will fossil fuel reserves be diminished ?," vol. 37, pp. 181–189, 2009, doi: 10.1016/j.enpol.2008.08.016.

[3] B. Zohuri, *Nuclear fuel cycle and decommissioning*. Elsevier Ltd., 2020. doi: 10.1016/B978-0-12-818483-7.00002-0.

[4] O. Edenhofer *et al.*, *Renewable energy sources and climate change mitigation: Special report of the intergovernmental panel on climate change*. 2011. doi: 10.1017/CBO9781139151153.

[5] I. To and S. Energy, "INTRODUCTION," pp. 1–48.

[6] M. Ehikhamenle and R. O. Okeke, "Design and Development of 2 . 5KVA Inverter Adopting a Microcontroller Based Frequency Meter," vol. 3, no. 1, 2017.

[7] S. Edition, "The Authoritative Dictionary of IEEE Standards Terms," *IEEE Std 100-2000*, pp. 1–1362, 2000.

[8] T. L. Alumona, G. C. Nwalozie, S. U. Ufoaroh, and T. A. Alade, "Design and Construction of an RF Remote Control 5kva Inverter System," vol. 5, no. 4, pp. 570–583, 2016.

[9] V. K. Lohan, "Inverter and Other Applications of Power Electronics Inverter and Other Applications of Power Electronics," *IJEEMF Int. J. Electr. Electron. Mech. Fundam.*, vol. 02, no. 01, pp. 2278–3989, 2012.

[10] N. Evalina, A. Azis H, Rimbawati, and Cholish, "Efficiency analysis on the inverter using the energy-saving lamp," *IOP Conf. Ser. Mater. Sci. Eng.*, vol. 674, no. 1, 2019, doi: 10.1088/1757-899X/674/1/012034.

[11] "Design Methodology of Off-Grid PV Solar Powered System (A Case Study of Solar Powered Bus Shelter) Author : Ayaz A . Khamisani Advisors : Dr . Peter Ping Liu , Dr . Jerry Cloward , Dr . Rendong Bai Table of content".

[12] F. Kazhamiaka, C. Rosenberg, and S. Keshav, "Practical Strategies for Storage Operation in Energy Systems: Design and Evaluation," *IEEE Trans. Sustain. Energy*, vol. 7, no. 4, pp. 1602–1610, 2016, doi: 10.1109/TSTE.2016.2569425.

[13] A. Trzynadlowski, *Modern Power Electronics*, vol. 18, no. 7. 2005. doi: 10.1109/mper.1998.686953.

[14] M. Nassereddine *et al.*, "Stand Alone PV House Design for Maximum Power Output in Sydney Australia Metropolitan Area," *MATEC Web Conf.*, vol. 171, pp. 1–6, 2018, doi: 10.1051/matecconf/201817101001.

[15] M. Patel and Z. Zhou, "An Interleaved Battery Charger Circuit for a Switched Capacitor Inverter-Based Standalone Single-Phase Photovoltaic Energy Management System," *Energies*, vol. 16, no. 20, 2023, doi: 10.3390/en16207155.

[16] M. Nassereddine, J. Rizk, M. Nagrial, and A. Hellany, "Battery sustainable PV solar house: Storage consideration for off grid," *3rd Int. Conf. Electr. Biomed. Eng. Clean Energy Green Comput. EBECEGC 2018*, no. 1, pp. 34–38, 2018, doi: 10.1109/EBECEGC.2018.8357129.

[17] B. A. Sinha and S. S. Sahu, "MPPT CONTROL Of STANDALONE -PV SYSTEM With BATTERY as an ENERGY STORAGE ELEMENT".

[18] M. M. Yawale, "Maximum Power Point Tracking of Isolated Solar System," *Int. J. Res. Appl. Sci. Eng. Technol.*, vol. 6, no. 4, pp. 2278–2282, 2018, doi: 10.22214/ijraset.2018.4389.

[19] S. Roy, P. K. Sahu, and S. Jena, "Analysis and control strategy of standalone PV system with various reference frames," *Open Eng.*, vol. 12, no. 1, pp. 616–626, 2022, doi: 10.1515/eng-2022-0371.

[20] R. Zamodzki, C. M. O. Stein, E. G. Carati, J. P. Da Costa, and R. Cardoso, "Stability analysis of three-phase stand-alone inverters with LCL filter," *2016 12th IEEE Int. Conf. Ind. Appl. INDUSCON 2016*, 2017, doi: 10.1109/INDUSCON.2016.7874586.

[21] F. Andrade, K. Kampouropoulos, J. Cusido, and L. Romeral, "Stability analysis of a microgrid system based on inverter-interfaced distributed generators," *Adv. Electr. Comput. Eng.*, vol. 13, no. 3, pp. 17–22, 2013, doi: 10.4316/aece.2013.03003.

[22] M. Hosenuzzaman, N. A. Rahim, J. Selvaraj, M. Hasanuzzaman, A. B. M. A. Malek, and A. Nahar, "Global prospects, progress, policies, and environmental impact of solar photovoltaic power generation," *Renew. Sustain. Energy Rev.*, vol. 41, pp. 284–297, 2015, doi: 10.1016/j.rser.2014.08.046.

[23] R. Venugopal *et al.*, "Review on Unidirectional Non-Isolated High Gain DC-DC Converters for EV Sustainable DC Fast Charging Applications," *IEEE Access*, vol. 11, no. August, pp. 78299–78338, 2023, doi: 10.1109/ACCESS.2023.3276860.

[24] P. Lakshmipriya and K. J. R. Thomas, "Unidirectional DC / DC Converter for Microgrids," no. May, pp. 74–76, 2019.

[25] O. Oladepo and G. A. Adegboyega, "Development and Implementation of High Efficiency Inverter System for Industrial use," vol. 3, no. 3, pp. 381–390, 2011, [Online]. Available: http://www.ripublication.com/Volume/ijeerv3n3.htm

[26] S. S. Mukrimaa *et al.*, "No 主観的健康感を中心とした在宅高齢者における 健康関連指標に関する共分散構造分析Title," *J. Penelit. Pendidik. Guru Sekol. Dasar*, vol. 6, no. August, p. 128, 2016.

[27] L. S. Czarnecki, "of the Instantaneous Reactive Power p - q Theory," *Power*, vol. 19, no. 3, pp. 828–836, 2004.

[28] V. Salas, W. Suponthana, and R. A. Salas, "Overview of the off-grid photovoltaic diesel batteries systems with AC loads," *Appl. Energy*, vol. 157, pp. 195–216, 2015, doi: 10.1016/j.apenergy.2015.07.073.

[29] S. B. Kjaer, J. K. Pedersen, and F. Blaabjerg, "A review of single-phase grid-connected inverters for photovoltaic modules," *IEEE Trans. Ind. Appl.*, vol. 41, no. 5, pp. 1292–1306, 2005, doi: 10.1109/TIA.2005.853371.

[30] F. Nejabatkhah and Y. W. Li, "Overview of Power Management Strategies of Hybrid AC/DC Microgrid," *IEEE Trans. Power Electron.*, vol. 30, no. 12, pp. 7072–7089, 2015, doi: 10.1109/TPEL.2014.2384999.

[31] R. O. Cáceres and I. Barbi, "A boost DC-AC converter: Analysis, design, and experimentation," *IEEE Trans. Power Electron.*, vol. 14, no. 1, pp. 134–141, 1999, doi: 10.1109/63.737601.

[32] M. Hasan, J. Maqsood, M. Q. Baig, S. M. A. S. Bukhari, and S. Ahmed, "Design and Implementation of Single Phase Pure Sine Wave Inverter Using Multivibrator IC," *Proc. - UKSim-AMSS 17th Int. Conf. Comput. Model. Simulation, UKSim 2015*, pp. 451–455, 2016, doi: 10.1109/UKSim.2015.58.

[33] E. Yan and M. Menéndez, "H-Bridges".

[34] M. A. H. Alshehri and Y. Guo, "Energy Management Strategies of Grid-Connected Microgrids under Different Reliability Conditions," 2023.

[35] S. H. Kim, B. J. Kim, and C. Y. Won, "A Study on Decentralized Inverse-Droop Control for Input Voltage Sharing of ISOP Converter in the Current Control Loop," *ICPE 2019 - ECCE Asia - 10th Int. Conf. Power Electron. - ECCE Asia*, pp. 2382–2387, 2019, doi: 10.23919/icpe2019-ecceasia42246.2019.8797085.

[36] L. Kerachev, A. Andreta, Y. Lembeye, and J. C. Crébier, "Generic approach for design, configuration and control of modular converters," *PCIM Eur. 2017 - Int. Exhib. Conf. Power Electron. Intell. Motion, Renew. Energy Energy Manag.*, no. May, pp. 16–18, 2017, doi: 10.1109/SBMicro.2017.7990692.

[37] T. Lamorelle, S. Nguyen, J. C. Podvin, D. Rubio, Y. Lembeye, and J. C. Crébier, "Multi-cell DC-DC converters - Input differential mode filtering generic design rules and

implementation," *PCIM Eur. Conf. Proc.*, no. May, pp. 616–623, 2019.

[38] M. Kasper, D. Bortis, and J. W. Kolar, "Scaling and balancing of multi-cell converters," *2014 Int. Power Electron. Conf. IPEC-Hiroshima - ECCE Asia 2014*, pp. 2079–2086, 2014, doi: 10.1109/IPEC.2014.6869875.

[39] T. Lamorelle, Y. Lembeye, and J. C. Crebier, "Handling Differential Mode Conducted EMC in Modular Converters," *IEEE Trans. Power Electron.*, vol. 35, no. 6, pp. 5812–5819, 2020, doi: 10.1109/TPEL.2019.2947735.

[40] Z. Liang, F. C. Lee, G. Q. Lu, and D. Borojevic, "Embedded power-a multilayer integration technology for packaging of IPEMs and PEBBs," *IWIPP 2000 - Int. Work. Integr. Power Packag.*, pp. 41–45, 2000, doi: 10.1109/IWIPP.2000.885179.

[41] H. Malek, "Control of Grid-Connected Photovoltaic Systems Using Fractional Order Operators," p. 159, 2014.

[42] Z. Zeng, H. Yang, R. Zhao, and C. Cheng, "Topologies and control strategies of multi-functional grid-connected inverters for power quality enhancement: A comprehensive review," *Renew. Sustain. Energy Rev.*, vol. 24, pp. 223–270, 2013, doi: 10.1016/j.rser.2013.03.033.

[43] I. C. Emeji, O. M. Ama, U. O. Aigbe, K. Khoele, P. O. Osifo, and S. S. Ray, "Electrochemical Cells," *Eng. Mater.*, vol. 414, no. November, pp. 65–84, 2020, doi: 10.1007/978-3-030-43346-8_4.

[44] P. Chuenchum, P. Suttinon, and P. Ruangrassamee, "Assessment of cross-sectoral damage from water deficits under changing climate and regional development in Nan River Basin, Thailand," *World Environ. Water Resour. Congr. 2017 Int. Perspect. Hist. Heritage, Emerg. Technol. Student Pap. - Sel. Pap. from World Environ. Water Resour. Congr. 2017*, pp. 694–709, 2017, doi: 10.1061/9780784480595.062.

[45] G. Li *et al.*, "High-efficiency solution processable polymer photovoltaic cells by self-organization of polymer blends," *Nat. Mater.*, vol. 4, no. 11, pp. 864–868, 2005, doi:

10.1038/nmat1500.

[46] K. M. Coakley and M. D. McGehee, “Photovoltaic cells made from conjugated polymers infiltrated into mesoporous titania,” *Appl. Phys. Lett.*, vol. 83, no. 16, pp. 3380–3382, 2003, doi: 10.1063/1.1616197.

[47] A. Kojima, K. Teshima, Y. Shirai, and T. Miyasaka, “Organometal halide perovskites as visible-light sensitizers for photovoltaic cells,” *J. Am. Chem. Soc.*, vol. 131, no. 17, pp. 6050–6051, 2009, doi: 10.1021/ja809598r.

[48] B. C. O’Regan and F. Lenzmann, “Charge Transport and Recombination in a Nanoscale Interpenetrating Network of n-Type and p-Type Semiconductors: Transient Photocurrent and Photovoltage Studies of TiO2/ Dye/CuSCN Photovoltaic Cells,” *J. Phys. Chem. B*, vol. 108, no. 14, pp. 4342–4350, 2004, doi: 10.1021/jp035613n.

[49] M. Mahija, “Regenerative Braking System in Electric Vehicles using Induction Motor,” vol. 7, no. 5, pp. 722–730, 2022.

[50] M. Kumar, S. K. Morla, and R. N. Mahanty, “Modeling and simulation of a Micro-grid connected with PV solar cell its protection strategy,” *2019 4th IEEE Int. Conf. Recent Trends Electron. Information, Commun. Technol. RTEICT 2019 - Proc.*, pp. 146–150, 2019, doi: 10.1109/RTEICT46194.2019.9016924.

[51] H. A. Alharkan, “A control algorithm for the solar village microgrid system,” 2016, [Online]. Available: https://scholarsmine.mst.edu/masters_thesesTheses.7544.https://scholarsmine.mst.edu/masters_theses/7544

[52] R. Hayler, “Post- to pre-tax discount rates: Not a simple conversion,” *J. Bus. Valuat. Econ. Loss Anal.*, vol. 14, no. 1, pp. 1–7, 2019, doi: 10.1515/jbvela-2018-0013.

[53] K. N. Hasan, M. E. Haque, M. Negnevitsky, and K. M. Muttaqi, “Control of energy storage interface with a bidirectional converter for photovoltaic systems,” *2008 Australas. Univ. Power Eng. Conf. AUPEC 2008*, no. May 2014, 2008.

[54] S. Adhikari and F. Li, "Coordinated V-f and P-Q control of solar photovoltaic generators with MPPT and battery storage in microgrids," *IEEE Trans. Smart Grid*, vol. 5, no. 3, pp. 1270–1281, 2014, doi: 10.1109/TSG.2014.2301157.

[55] S. Adhikari, "TRACE : Tennessee Research and Creative Exchange Control of Solar Photovoltaic (PhV) Power Generation In Grid- connected and Islanded Microgrids," 2013.

[56] S. Hussain Basha and P. Venkatesh, "Control of Solar Photovoltaic (Pv) Power Generation in Grid-Connected and Islanded Microgrids," *Int. J. Eng. Reseaerch Gen. Sci.*, vol. 3, no. 3, pp. 121–141, 2015.

[57] L. E, B. R, P. F, T. H.A., and W. S, "Multiphase induction motor drives-a technology status review," *IET Electr. Power Appl.*, vol. 1, no. 5, pp. 643–656, 2007, doi: 10.1049/iet-epa.

[58] H. Akagi, Y. Kanazawa, and A. Nabae, "Instantaneous Reactive Power Compensators Comprising Switching Devices without Energy Storage Components," *IEEE Trans. Ind. Appl.*, vol. IA-20, no. 3, pp. 625–630, 1984, doi: 10.1109/TIA.1984.4504460.

[59] R. S. Herrera, P. Salmerón, J. R. Vázquez, S. P. Litrán, and A. Pérez, "Generalized instantaneous reactive power theory in poly-phase power systems," *2009 13th Eur. Conf. Power Electron. Appl. EPE '09*, 2009.

[60] M. V. S. Sivakrishna and K. S. S. Prasad Raju, "Comparison of control strategies for shunt active power filter in distribution systems," *Int. J. Recent Technol. Eng.*, vol. 8, no. 1, pp. 124–130, 2019.

[61] A. K. Yadav, P. Gaur, S. K. Jha, J. R. P. Gupta, and A. P. Mittal, "Optimal speed control of hybrid electric vehicles," *J. Power Electron.*, vol. 11, no. 4, pp. 393–400, 2011, doi: 10.6113/JPE.2011.11.4.393.

[62] H. Rasool, A. Mutal, A. Rasool, W. Ahmad, and A. A. Ikram, "MPPT based ASBC controller and solar panel monitoring system," *2014 Int. Conf. Energy Syst. Policies,*

ICESP 2014, 2015, doi: 10.1109/ICESP.2014.7347002.

[63] A. Dutta, N. Barua, and A. Saha, "Design of an arduino based maximum power point tracking (MPPT) solar charge controller," *BRAC Univ.*, no. February, pp. 1–72, 2016, doi: 10.13140/RG.2.2.13850.93124.

[64] Z. Cai, "Digital Commons @ DU Digital Commons @ DU Design and Control of Islanded Microgrid Design and Control of Islanded Microgrid," 2016, [Online]. Available: https://digitalcommons.du.edu/etd/1226

[65] F. Habashi, "Reactive metals and the periodic table," *Light Met. 1992*, pp. 1279–1286, 1992.

[66] E. Engineering, "Design of a Charge Controller Circuit with Maximum Power Point Tracker (MPPT) for Photovoltaic System," 2012.

[67] S. D'Arco, J. A. Suul, and O. B. Fosso, "Small-signal modelling and parametric sensitivity of a Virtual Synchronous Machine," *Proc. - 2014 Power Syst. Comput. Conf. PSCC 2014*, pp. 1–9, 2014, doi: 10.1109/PSCC.2014.7038410.

[68] J. Z. Zhou, H. Ding, S. Fan, Y. Zhang, and A. M. Gole, "Impact of short-circuit ratio and phase-locked-loop parameters on the small-signal behavior? of a VSC-HVDC converter," *IEEE Trans. Power Deliv.*, vol. 29, no. 5, pp. 2287–2296, 2014, doi: 10.1109/TPWRD.2014.2330518.

[69] "Transient Phenomena in Electrical Power Systems," *Transient Phenomena in Electrical Power Systems*. 1965. doi: 10.1016/c2013-0-08253-9.

[70] R. L. W. Ii *et al.*, *LINEAR STATE-SPACE CONTROL SYSTEMS*. 2007.

[71] X. Liu, P. Wang, and P. C. Loh, "Optimal coordination control for stand-alone PV system with nonlinear load," *2010 9th Int. Power Energy Conf. IPEC 2010*, pp. 104–109, 2010, doi: 10.1109/IPECON.2010.5697139.

[72] C. Pham, T. Kerekes, and R. Teodorescu, "High efficient bidirectional battery converter

for residential PV systems," *Proc. - 2012 3rd IEEE Int. Symp. Power Electron. Distrib. Gener. Syst. PEDG 2012*, pp. 890–894, 2012, doi: 10.1109/PEDG.2012.6254106.

[73] C. J. Rydh and B. A. Sandén, "Energy analysis of batteries in photovoltaic systems. Part I: Performance and energy requirements," *Energy Convers. Manag.*, vol. 46, no. 11–12, pp. 1957–1979, 2005, doi: 10.1016/j.enconman.2004.10.003.

[74] P. R. Geffe, "LC Filter Design," *CRC Handb. Electr. FILTERS*, no. November, pp. 45–79, 2020, doi: 10.1201/9781003069201-5.

[75] G. Szentirmai, *Electronic filter design handbook*, vol. 70, no. 3. 2008. doi: 10.1109/proc.1982.12308.

[76] M. Shao, R. Liu, and D. Lv, "Control strategy of voltage and frequency for islanded microgrid," *Conf. Proc. - 2012 IEEE 7th Int. Power Electron. Motion Control Conf. - ECCE Asia, IPEMC 2012*, vol. 3, pp. 2085–2089, 2012, doi: 10.1109/IPEMC.2012.6259165.